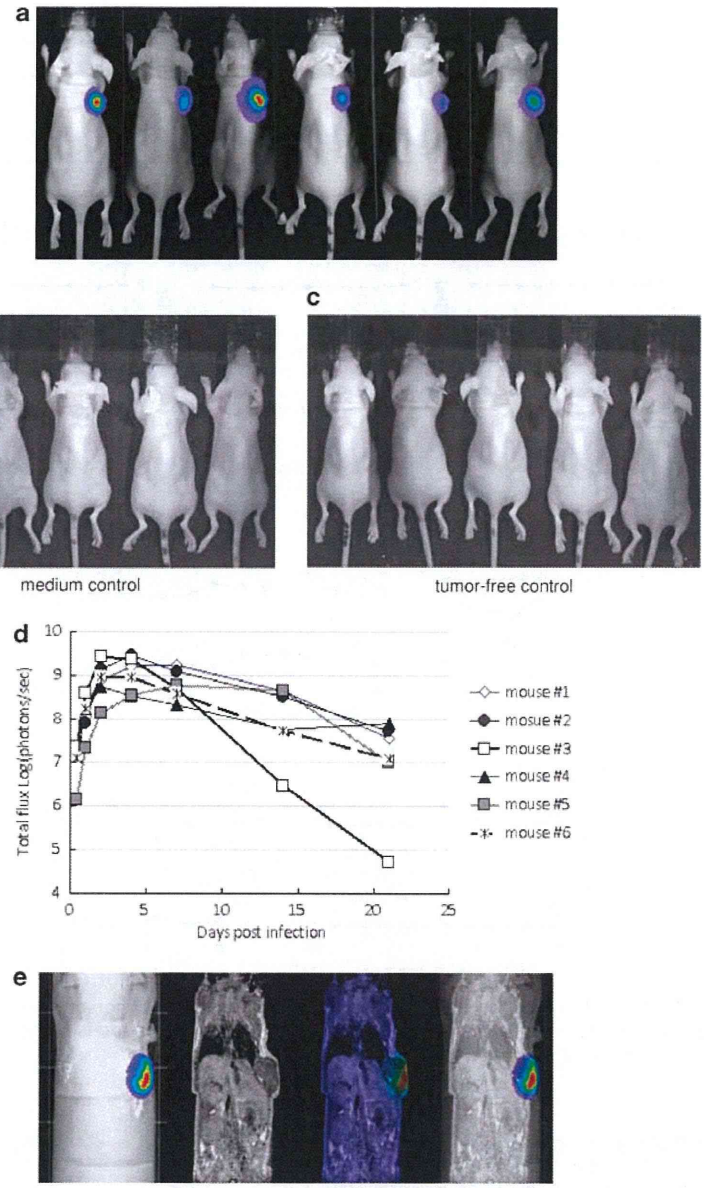

Figure 6. Localization of rMV-luc-SLAMblind in xenografted mice. (**a**) Nude mice bearing subcutaneous MDA-MB-453 tumor intratumorally administered with rMV-luc-SLAMblind. Luciferase signals were analyzed by BLI at 2 d.p.i. (**b**) BLI of medium control mice at 2 d.p.i. (**c**) BLI of tumor-free control mice at 2 d.p.i. (**d**) The level of luciferase expression measured at each time point. (**e**) A fusion image of BLI and MRI in a mouse at 10 d.p.i. From left to right in the panel: the BLI overlaid on the photographic image, MRI, fusion image of blended BLI and MRI, and fusion image of overlaid BLI and MRI.

St Louis, MO, USA) with 5% FBS. BHK cells were grown in Dulbecco's Modified Eagle's Medium (Sigma-Aldrich) with 5% FBS. NHDFs were purchased from Cell Systems (Kirkland, WA, USA) and maintained in CS-C medium (Cell Systems) supplemented with CSC growth factor (Cell Systems) and 5% FBS.

Recovery of recombinant MVs

The pMV-HL(7+) plasmid encodes the full-length antigenomic cDNA of MV HL wild-type strain.[23] The pMV-EGFP and pMV-LUC, which have an additional transcription unit encoding EGFP and firefly luciferase (luc) genes, have been reported previously.[23,45] The R533A substitution was introduced into pMV-HL(7+), pMV-EGFP and pMV-LUC by site-directed mutagenesis and the resultant plasmids were designated as pMV-SLAMblind, pMV-EGFP-SLAMblind and pMV-luc-SLAMblind, respectively. The plasmid p(+)MV2A (a gift from MA Billeter) encodes the full-length antigenomic cDNA of the Edmonston B vaccine strain.[47] We found that the p(+)MV2A had the following nucleotide differences from the reported sequence data for the Edmonston B strain (GenBank accession no. Z66517): A3310G, C3627T, C4708T, T5703A, A5737G, C6414T, A6477G, T6546C, T7023C, T8353C, A8721C and A8745G. Five of them caused amino-acid changes in the P (M502V), M (P64S), F (M97V) and H (N484T and E492G) proteins.

The recombinant MV HL (rMV) and rMV-EGFP were recovered as described previously.[23] To recover SLAM-blind recombinant MVs, MCF7 cells were used for virus amplification owing to the restricted receptor usage of the virus. The rescued virus from p(+)MV2A was referred to as rMV-Edmonston. To recover rMV-Edmonston, Vero cells were used for virus amplification.

Virus titers

Virus titers were determined as 50% tissue culture infectious dose ($TCID_{50}$) by the Reed–Muench method.[48] The titers of SLAM-blind recombinant MVs

a

Monkey	Clinical Signs			Viremia ([Log [$TCID_{50}/10^5$ PBMCs])				
	Rash	Anorexia	Diarrhea	2dpi	4dpi	7dpi	14dpi	21dpi
Cynomolgous monkey	No	No	No	<1	<1	<1	<1	<1
Rhesus monkey #1	No	No	No	<1	<1	<1	<1	n.d.
Rhesus monkey #2	No	No	No	<1	<1	<1	<1	n.d.

n.d. : not determined

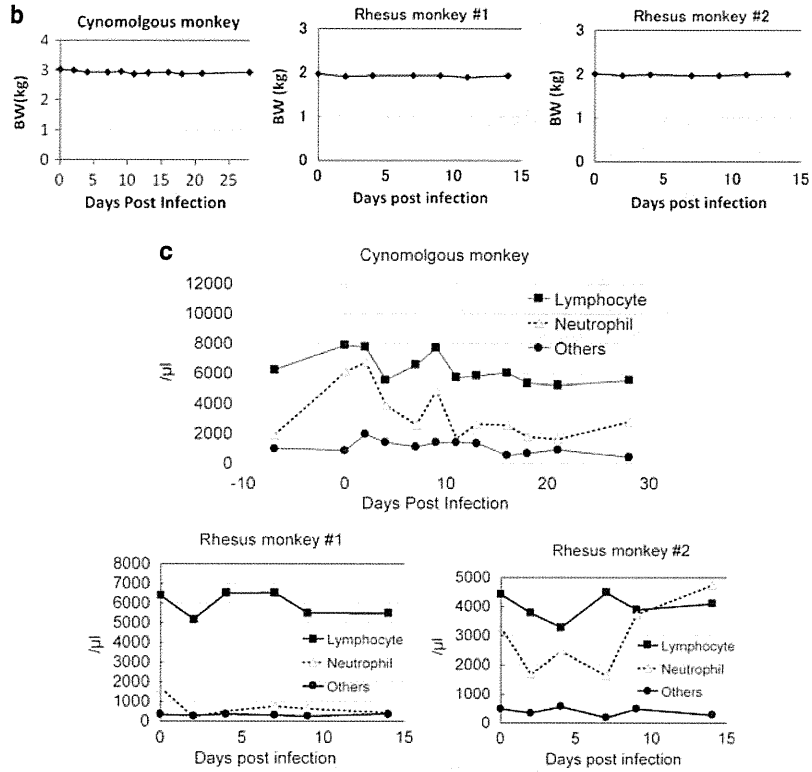

Figure 7. Safety study of rMV-SLAMblind in monkeys. One cynomolgus and two rhesus monkeys were subcutaneously inoculated with 10^6 $TCID_{50}$ of rMV-SLAMblind. (**a**) Clinical signs observed and virus levels in PBMCs determined in the monkeys. Body weight (**b**) and blood leukocyte number (**c**) were measured at each time point.

could be determined only in PVRL4-expressing cells, owing to receptor usage restriction, and were therefore titrated in MCF7 cells. MV infection in MCF7 cells was detected by fluorescence of EGFP or indirectly by immunostaining using anti-N protein monoclonal antibody (MAb) 8G[49] as a primary antibody and Alexa-Fluor-488-conjugated anti-mouse antibody (Invitrogen) as a secondary antibody. We note that titers of rMV and rMV-EGFP determined in MCF7 cells were similar to those determined in B95a cells, and titers of rMV-Edmonston determined in MCF7 cells were similar to those determined in Vero cells.

RT-PCR analysis

Total RNA was extracted from cells using ISOGEN (Nippon Gene, Tokyo, Japan) and 2 μg total RNA was reverse transcribed using PrimeScript RTase (Takara, Shiga, Japan) by random hexamer priming. The resultant cDNA was PCR-amplified using Thermo-start Taq DNA polymerase (ABgene, Epsom, UK) with primer pairs specific for SLAM or glyceraldehyde 3-phosphate dehydrogenase (GAPDH) mRNA. PCR amplicons were visualized on agarose gels.

Growth kinetics

Monolayers of MCF7 cells in 12-well plates were infected with recombinant MVs at an MOI of 0.01 and incubated in RPMI medium supplemented with 5% FCS. At various time points, released virus was obtained from the culture supernatants, and cell-associated virus was recovered from infected cells by three cycles of freezing–thawing. Virus titers were determined in MCF7 cells.

Infection inhibition assay using antibodies

Monolayers of MCF7, MDA-MB-453, SKBR3 and Vero cells in 96-well plates were pretreated for 1 h at 37 °C with medium containing 10 μg ml^{-1} of anti-human CD46 MAb (clone M177; HyCult Biotechnology, Uden, The Netherlands)[50] or anti-human PVRL4 goat polyclonal antibody (R&D Systems, Minneapolis, MN, USA). Control monolayers of the four cell lines were similarly treated with medium lacking the antibodies. Cells were infected with rMV-EGFP, rMV-EGFP-SLAMblind or rMV-Edmonston at an MOI of 0.1. After infection, cells were incubated in medium either containing or lacking the antibodies. Cells infected with rMV-Edmonston were detected by immunostaining using anti-N rabbit polyclonal antibody. Cells were observed under a fluorescent microscope at 2 (Vero) or 3 d.p.i. (the others).

Infection assay on cells transfected with plasmids expressing CD46 and PVRL4

Human CD46 cDNA (C2 isoform) and human PVRL4 cDNA were obtained by RT-PCR of total RNA from 293 and MCF7 cells, respectively. The cDNAs were subcloned into pCAGGS.[51] The resultant plasmids were designated pCAG-hCD46 and pCAG-hPVRL4.

For the transfection of pCAG-hCD46, CHO-K1 cells were seeded in a 6-well plate and were transfected with either pCAG-hCD46 or pCAGGS.

After overnight incubation, the cells were detached from the plate by trypsin treatment and seeded in a 96-well plate. On the following day, cells were infected with rMV-SLAMblind or rMV-Edmonston at an MOI of 1 for 1 h at 37 °C. The virus inoculum was replaced with medium containing fusion inhibitory peptide (z-D-Phe-Phe-Gly; Sigma-Aldrich) to prevent cell–cell fusion and infection by virus progeny. Incubation was continued at 37 °C for 2 days and cells were fixed with 4% paraformaldehyde and immunostained using anti-N MAb. The number of infected cells per well was counted under a fluorescent microscope. Relative infectivity in cells transfected with pCAG-hCD46 or pCAGGS was calculated as the mean of triplicate counts divided by the mean of triplicate counts in cells transfected with pCAGGS and was expressed as a percentage.

For transfection of pCAG-hPVRL4, we used BHK cells because CHO-K1 cells died after transfection with pCAG-hPVRL4. BHK cells were transfected with pCAG-hPVRL4 or pCAGGS as described above and infected with rMV-SLAMblind or rMV-Edmonston at an MOI of 0.1. Relative infectivity in cells transfected with pCAG-hPVRL4 or pCAGGS was determined as above.

WST-1 assay

Cell viability was determined using a WST-1 Cell Proliferation kit (Takara) according to the manufacturer's protocol. Monolayers of cells in 96-well plates were infected with recombinant MVs at different MOIs. Culture medium was changed at 3, 5 and 7 d.p.i. Cell viability was measured by absorbance at 450 nm on a Microplate reader model 450 (Bio-Rad, Hercules, CA, USA). The viability of cells infected with virus was calculated as the mean of triplicate absorbance values divided by the mean of triplicate absorbance values of uninfected cells and was expressed as a percentage.

Assessment of *in vivo* oncolytic activity

All animal experiments were approved by the Experimental Animal Committee of The University of Tokyo. Six-week-old female severe combined immune deficiency mice were purchased from Clea Japan (Tokyo, Japan). MCF7 cells (1.5×10^6) or MDA-MB-453 cells (3×10^6) were suspended in 50 μl PBS and the suspension was mixed with 50 μl of Matrigel HC (BD Biosciences, San Diego, CA, USA) before subcutaneous injection. For the MCF7 group, mice were administered intratumorally with 10^5 $TCID_{50}$ of rMV-SLAMblind ($n=5$), rMV-Edmonston ($n=5$) or Opti-MEM (Invitrogen) ($n=5$) at 6 days post implantation. Virus administration was repeated at 3 and 19 d.p.i. For the MDA-MB-453 group, mice were administered intratumorally with 10^6 $TCID_{50}$ of rMV-SLAMblind ($n=9$), rMV-Edmonston ($n=9$) or Opti-MEM ($n=8$) at 14 days post implantation. Virus administration was repeated at 14 d.p.i. Tumor diameters were measured with calipers. Tumor volume was calculated based on the formula (width × width × length)/2.

Visualization of *in vivo* infection of MDA-MB-453 xenografts by recombinant MV

Six-week-old female BALB/c nude mice were purchased from Clea Japan. A total of 11 mice were subcutaneously implanted with MDA-MB-453 cells as described above. Five mice were injected with a cell-free PBS/Matrigel mixture (tumor-free control). At 14 days post implantation, the mice received a single intratumoral injection of 10^6 $TCID_{50}$ of rMV-luc-SLAMblind or Opti-MEM (medium control). *In vivo* BLI was performed at 10 h post infection, and 1, 2, 4, 7, 14 and 21 d.p.i. Before each imaging, mice received a subcutaneous injection[52] of 3 mg of D-luciferin (Gold Biotechnology, St Louis, MO, USA) diluted in 200 μl PBS. Images were acquired about 15 min after luciferin administration using the Xenogen Ivis 100 System (Xenogen/Caliper Life Sciences, Alameda, CA, USA). The Ivis 100 cooled CCD camera system was used for emitted light acquisition. Imaging parameters were an exposure time of 1–60 s, binning of 4 or 8 and field of view of 15 cm. Luciferase activity was analyzed using Living Image Software (version 2.5; Xenogen), according to the manufacturer's instructions. The level of firefly luciferase was expressed as photons s^{-1} cm^{-2}. Fusion images of BLI and MRI were acquired as described previously.[25]

Inoculation of rMV-SLAMblind into monkeys

A 4-year-old female cynomolgus monkey (*Macaca fascicularis*) and two 15-month-old male rhesus monkeys (*Macaca mulatta*) were obtained from Japan Wild Animal Research (Kagoshima, Japan) and were confirmed as seronegative for MV. The monkeys were inoculated subcutaneously with 10^6 $TCID_{50}$ of rMV-SLAMblind.

Leukocyte numbers

In all, 100 μl of peripheral blood was collected at various time points. Leukocyte numbers were counted using an automated hematological analyzer (model KX-21NV; Sysmex, Kobe, Japan). The percentages of lymphocytes, neutrophils, eosinophils, basophils and monocytes were determined on a Giemsa-stained thin blood smear.

Virus levels in PBMCs

In all, 2 ml of peripheral blood was collected at 2, 4, 7, 14 and 21 d.p.i. The blood was diluted to 10 ml in PBS, layered on 3 ml of gradient separation medium (49.2% Percoll and 150 mM NaCl) and centrifuged at 400 × *g* for 30 min at room temperature. PBMCs were recovered at the interface. After washing twice with PBS, cells were resuspended in 2 ml RPMI medium. Virus levels were quantified by end-point dilution coculture with MCF7 cells. Serial 10-fold dilutions of PBMCs were made in RPMI medium supplemented with 5% FBS. Four replicates of PBMCs were cocultured with MCF7 cells in 96-well plates. The cultures were maintained for 7 days and immunostained using anti-N MAb for virus titration.

Flow cytometry

Cells were stripped with 2 mM EDTA and then pelleted by centrifugation at 200 × *g*. The pelleted cells were resuspended in sample buffer (PBS with 1% bovine serum albumin and 0.02% NaN_3). Cells (10^6) were incubated with 0.5 μg of primary antibody in 100 μl of sample buffer on ice for 30 min. The following antibodies were used as primary antibodies: anti-human SLAM MAb (clone 7D4; Biolegend, San Diego, CA, USA), anti-human CD46 MAb, anti-PVRL4 goat polyclonal antibody (R&D Systems), mouse control IgG1 (R&D Systems) and goat control IgG (R&D Systems). Cells were washed once with PBS and incubated with 0.1 μg of Alexa-488-conjugated anti-mouse or anti-goat antibody (Invitrogen) in 100 μl of sample buffer on ice for 30 min. After being washed twice with PBS, cells were fixed with 4% paraformaldehyde and analyzed on a BD FACSCalibur (BD Biosciences).

CONFLICT OF INTEREST

The authors declare no conflict of interest.

ACKNOWLEDGEMENTS

We thank Dr MA Billeter (University of Zurich) for kindly providing p(+)MV2A plasmid. This work was supported by Grants-in-Aid for Scientific Research (KAKENHI) from Japan Society for the Promotion of Science (JSPS), Japan, and in part by Global COE Program 'Center of Education and Research for the Advanced Genome-Based Medicine: For personalized medicine and the control of worldwide infectious diseases', MEXT, Japan.

REFERENCES

1 Jemal A, Bray F, Center MM, Ferlay J, Ward E, Forman D. Global cancer statistics. *CA Cancer J Clin* 2011; **61**: 69–90.
2 Roche H, Vahdat LT. Treatment of metastatic breast cancer: second line and beyond. *Ann Oncol* 2011; **22**: 1000–1010.
3 Bourke MG, Salwa S, Harrington KJ, Kucharczyk MJ, Forde PF, de Kruijf M *et al.* The emerging role of viruses in the treatment of solid tumours. *Cancer Treat Rev* 2011; **37**: 618–632.
4 Griffin DE. Measles virus. In: David M, Knipe P, Peter M, Howley M, Griffin DE, Lamb RA, Malcolm A, Martin M, Bernard Roizman S, Stephen E, Straus M (eds). *Fields Virology*. Lippincott Williams & Wilkins: Philadelphia, 2006, pp 1401–1586.
5 Msaouel P, Iankov ID, Allen C, Morris JC, von Messling V, Cattaneo R *et al.* Engineered measles virus as a novel oncolytic therapy against prostate cancer. *Prostate* 2009; **69**: 82–91.
6 Allen C, Paraskevakou G, Liu C, Iankov ID, Msaouel P, Zollman P *et al.* Oncolytic measles virus strains in the treatment of gliomas. *Expert Opin Biol Ther* 2008; **8**: 213–220.
7 McDonald CJ, Erlichman C, Ingle JN, Rosales GA, Allen C, Greiner SM *et al.* A measles virus vaccine strain derivative as a novel oncolytic agent against breast cancer. *Breast Cancer Res Treat* 2006; **99**: 177–184.
8 Blechacz B, Splinter PL, Greiner S, Myers R, Peng KW, Federspiel MJ *et al.* Engineered measles virus as a novel oncolytic viral therapy system for hepatocellular carcinoma. *Hepatology* 2006; **44**: 1465–1477.
9 Sidorenko SP, Clark EA. Characterization of a cell surface glycoprotein IPO-3, expressed on activated human B and T lymphocytes. *J Immunol* 1993; **151**: 4614–4624.

10 Cocks BG, Chang CC, Carballido JM, Yssel H, de Vries JE, Aversa G. A novel receptor involved in T-cell activation. *Nature* 1995; **376**: 260–263.
11 Tatsuo H, Ono N, Tanaka K, Yanagi YSLAM. (CDw150) is a cellular receptor for measles virus. *Nature* 2000; **406**: 893–897.
12 Dorig RE, Marcil A, Chopra A, Richardson CD. The human CD46 molecule is a receptor for measles virus (Edmonston strain). *Cell* 1993; **75**: 295–305.
13 Liszewski MK, Post TW, Atkinson JP. Membrane cofactor protein (MCP or CD46): newest member of the regulators of complement activation gene cluster. *Annu Rev Immunol* 1991; **9**: 431–455.
14 Noyce RS, Bondre DG, Ha MN, Lin LT, Sisson G, Tsao MS *et al.* Tumor cell marker PVRL4 (nectin 4) is an epithelial cell receptor for measles virus. *PLoS Pathog* 2011; **7**: e1002240.
15 Muhlebach MD, Mateo M, Sinn PL, Prufer S, Uhlig KM, Leonard VH *et al.* Adherens junction protein nectin-4 is the epithelial receptor for measles virus. *Nature* 2011; **480**: 530–533.
16 Reymond N, Fabre S, Lecocq E, Adelaide J, Dubreuil P, Lopez M. Nectin4/PRR4, a new afadin-associated member of the nectin family that trans-interacts with nectin1/PRR1 through V domain interaction. *J Biol Chem* 2001; **276**: 43205–43215.
17 Leonard VH, Sinn PL, Hodge G, Miest T, Devaux P, Oezguen N *et al.* Measles virus blind to its epithelial cell receptor remains virulent in rhesus monkeys but cannot cross the airway epithelium and is not shed. *J Clin Invest* 2008; **118**: 2448–2458.
18 Takano A, Ishikawa N, Nishino R, Masuda K, Yasui W, Inai K *et al.* Identification of nectin-4 oncoprotein as a diagnostic and therapeutic target for lung cancer. *Cancer Res* 2009; **69**: 6694–6703.
19 Derycke MS, Pambuccian SE, Gilks CB, Kalloger SE, Ghidouche A, Lopez M *et al.* Nectin 4 overexpression in ovarian cancer tissues and serum: potential role as a serum biomarker. *Am J Clin Pathol* 2010; **134**: 835–845.
20 Fabre-Lafay S, Monville F, Garrido-Urbani S, Berruyer-Pouyet C, Ginestier C, Reymond N *et al.* Nectin-4 is a new histological and serological tumor associated marker for breast cancer. *BMC Cancer* 2007; **7**: 73.
21 Vongpunsawad S, Oezgun N, Braun W, Cattaneo R. Selectively receptor-blind measles viruses: Identification of residues necessary for SLAM- or CD46-induced fusion and their localization on a new hemagglutinin structural model. *J Virol* 2004; **78**: 302–313.
22 Kobune F, Takahashi H, Terao K, Ohkawa T, Ami Y, Suzaki Y *et al.* Nonhuman primate models of measles. *Lab Anim Sci* 1996; **46**: 315–320.
23 Terao-Muto Y, Yoneda M, Seki T, Watanabe A, Tsukiyama-Kohara K, Fujita K *et al.* Heparin-like glycosaminoglycans prevent the infection of measles virus in SLAM-negative cell lines. *Antiviral Res* 2008; **80**: 370–376.
24 Allen C, Vongpunsawad S, Nakamura T, James CD, Schroeder M, Cattaneo R *et al.* Retargeted oncolytic measles strains entering via the EGFRvIII receptor maintain significant antitumor activity against gliomas with increased tumor specificity. *Cancer Res* 2006; **66**: 11840–11850.
25 Inoue Y, Masutani Y, Kiryu S, Haishi T, Watanabe M, Tojo A *et al.* Integrated imaging approach to tumor model mice using bioluminescence imaging and magnetic resonance imaging. *Mol Imaging* 2010; **9**: 163–172.
26 Sato H, Kobune F, Ami Y, Yoneda M, Kai C. Immune responses against measles virus in cynomolgus monkeys. *Comp Immunol Microbiol Infect Dis* 2008; **31**: 25–35.
27 Takeda M, Takeuchi K, Miyajima N, Kobune F, Ami Y, Nagata N *et al.* Recovery of pathogenic measles virus from cloned cDNA. *J Virol* 2000; **74**: 6643–6647.
28 El Mubarak HS, Yuksel S, van Amerongen G, Mulder PG, Mukhtar MM, Osterhaus AD *et al.* Infection of cynomolgus macaques (Macaca fascicularis) and rhesus macaques (Macaca mulatta) with different wild-type measles viruses. *J Gen Virol* 2007; **88**: 2028–2034.
29 Zhu YD, Heath J, Collins J, Greene T, Antipa L, Rota P *et al.* Experimental measles. II. Infection and immunity in the rhesus macaque. *Virology* 1997; **233**: 85–92.
30 Yanagi Y, Takeda M, Ohno S, Seki F. Measles virus receptors and tropism. *Jpn J Infect Dis* 2006; **59**: 1–5.
31 de Swart RL, Ludlow M, de Witte L, Yanagi Y, van Amerongen G, McQuaid S *et al.* Predominant infection of CD150+ lymphocytes and dendritic cells during measles virus infection of macaques. *PLoS Pathog* 2007; **3**: e178.
32 Leonard VH, Hodge G, Reyes-Del Valle J, McChesney MB, Cattaneo R. Measles virus selectively blind to signaling lymphocytic activation molecule (SLAM; CD150) is attenuated and induces strong adaptive immune responses in rhesus monkeys. *J Virol* 2010; **84**: 3413–3420.
33 Jurianz K, Ziegler S, Garcia-Schuler H, Kraus S, Bohana-Kashtan O, Fishelson Z *et al.* Complement resistance of tumor cells: basal and induced mechanisms. *Mol Immunol* 1999; **36**: 929–939.
34 Anderson BD, Nakamura T, Russell SJ, Peng KW. High CD46 receptor density determines preferential killing of tumor cells by oncolytic measles virus. *Cancer Res* 2004; **64**: 4919–4926.
35 Liszewski MK, Atkinson JP. Membrane cofactor protein. *Curr Top Microbiol Immunol* 1992; **178**: 45–60.
36 Athanassiadou AM, Patsouris E, Tsipis A, Gonidi M, Athanassiadou P. The significance of Survivin and Nectin-4 expression in the prognosis of breast carcinoma. *Folia Histochem Cytobiol* 2011; **49**: 26–33.
37 Naniche D, Yeh A, Eto D, Manchester M, Friedman RM, Oldstone MB. Evasion of host defenses by measles virus: wild-type measles virus infection interferes with induction of Alpha/Beta interferon production. *J Virol* 2000; **74**: 7478–7484.
38 Ohno S, Ono N, Takeda M, Takeuchi K, Yanagi Y. Dissection of measles virus V protein in relation to its ability to block alpha/beta interferon signal transduction. *J Gen Virol* 2004; **85**: 2991–2999.
39 Takeda M, Ohno S, Tahara M, Takeuchi H, Shirogane Y, Ohmura H *et al.* Measles viruses possessing the polymerase protein genes of the Edmonston vaccine strain exhibit attenuated gene expression and growth in cultured cells and SLAM knock-in mice. *J Virol* 2008; **82**: 11979–11984.
40 Grote D, Russell SJ, Cornu TI, Cattaneo R, Vile R, Poland GA *et al.* Live attenuated measles virus induces regression of human lymphoma xenografts in immunodeficient mice. *Blood* 2001; **97**: 3746–3754.
41 Willmon C, Harrington K, Kottke T, Prestwich R, Melcher A, Vile R. Cell carriers for oncolytic viruses: Fed Ex for cancer therapy. *Mol Ther* 2009; **17**: 1667–1676.
42 Mader EK, Maeyama Y, Lin Y, Butler GW, Russell HM, Galanis E *et al.* Mesenchymal stem cell carriers protect oncolytic measles viruses from antibody neutralization in an orthotopic ovarian cancer therapy model. *Clin Cancer Res* 2009; **15**: 7246–7255.
43 Liu C, Russell SJ, Peng KW. Systemic therapy of disseminated myeloma in passively immunized mice using measles virus-infected cell carriers. *Mol Ther* 2010; **18**: 1155–1164.
44 Tahara M, Takeda M, Shirogane Y, Hashiguchi T, Ohno S, Yanagi Y. Measles virus infects both polarized epithelial and immune cells by using distinctive receptor-binding sites on its hemagglutinin. *J Virol* 2008; **82**: 4630–4637.
45 Watanabe A, Yoneda M, Ikeda F, Terao-Muto Y, Sato H, Kai C. CD147/EMMPRIN acts as a functional entry receptor for measles virus on epithelial cells. *J Virol* 2010; **84**: 4183–4193.
46 Kobune F, Sakata H, Sugiyama M, Sugiura A. B95a, a marmoset lymphoblastoid cell line, as a sensitive host for rinderpest virus. *J Gen Virol* 1991; **72**(Pt 3): 687–692.
47 Radecke F, Spielhofer P, Schneider H, Kaelin K, Huber M, Dotsch C *et al.* Rescue of measles viruses from cloned DNA. *EMBO J* 1995; **14**: 5773–5784.
48 Reed LJ, Muench H. A simple method of estimating fifty per cent endpoints. *Am J Hyg* 1938; **27**: 493–497.
49 Masuda M, Sato H, Kamata H, Katsuo T, Takenaka A, Miura R *et al.* Characterization of monoclonal antibodies directed against the canine distemper virus nucleocapsid protein. *Comp Immunol Microbiol Infect Dis* 2006; **29**: 157–165.
50 Iwata K, Seya T, Yanagi Y, Pesando JM, Johnson PM, Okabe M *et al.* Diversity of sites for measles virus binding and for inactivation of complement C3b and C4b on membrane cofactor protein CD46. *J Biol Chem* 1995; **270**: 15148–15152.
51 Niwa H, Yamamura K, Miyazaki J. Efficient selection for high-expression transfectants with a novel eukaryotic vector. *Gene* 1991; **108**: 193–199.
52 Inoue Y, Kiryu S, Izawa K, Watanabe M, Tojo A, Ohtomo K. Comparison of subcutaneous and intraperitoneal injection of D-luciferin for *in vivo* bioluminescence imaging. *Eur J Nucl Med Mol Imaging* 2009; **36**: 771–779.

IJC
International Journal of Cancer

An armed oncolytic herpes simplex virus expressing thrombospondin-1 has an enhanced *in vivo* antitumor effect against human gastric cancer

Toshiaki Tsuji[1], Mikihito Nakamori[1], Makoto Iwahashi[1], Masaki Nakamura[1], Toshiyasu Ojima[1], Takeshi Iida[1], Masahiro Katsuda[1], Keiji Hayata[1], Yasushi Ino[2], Tomoki Todo[2] and Hiroki Yamaue[1]

[1] Second Department of Surgery, Wakayama Medical University School of Medicine, 811-1 Kimiidera, Wakayama 641-8510, Japan
[2] Division of Innovative Cancer Therapy, The advanced Clinical Research Center, The Institute of Medical Science, The University of Tokyo, 4-6-1 Shirokanedai, Minato-ku, Tokyo 108-8639, Japan

Advanced gastric cancer is a common disease, but the conventional treatments are unsatisfactory because of the high recurrence rate. One of the promising new therapies is oncolytic virotherapy, using oncolytic herpes simplex viruses (HSVs). Thrombospondin-1 (TSP-1) suppresses tumor progression *via* multiple mechanisms including antiangiogenesis. Our approach to enhance the effects of oncolytic HSVs is to generate an armed oncolytic HSV that combines the direct viral oncolysis with TSP-1-mediated function for gastric cancer treatment. Using the bacterial artificial chromosome (BAC) system, a 3rd generation oncolytic HSV (T-TSP-1) expressing human TSP-1 was constructed for human gastric cancer treatment. The enhanced efficacy of T-TSP-1 was determined in both human gastric cancer cell lines *in vitro* and subcutaneous tumor xenografts of human gastric cancer cells *in vivo*. In addition, we examined the apoptotic effect of T-TSP-1 *in vitro*, and the antiangiogenic effect of T-TSP-1 *in vivo* compared with a non-armed 3rd generation oncolytic HSV, T-01. No apparent apoptotic induction by T-TSP-1 was observed for human gastric cancer cell lines TMK-1 cells but for MKN1 cells *in vitro*. Arming the viruses with TSP-1 slightly inhibited their replication in some gastric cancer cell lines, but the viral cytotoxicity was not attenuated. In addition, T-TSP-1 exhibited enhanced therapeutic efficacy and inhibition of angiogenesis compared with T-01 *in vivo*. In this study, we established a novel armed oncolytic HSV, T-TSP-1, which enhanced the antitumor efficacy by providing a combination of direct viral oncolysis with antiangiogenesis. Arming oncolytic HSVs may be a useful therapeutic strategy for gastric cancer therapy.

Gastric cancer currently ranks second in global cancer mortality.[1,2] Most patients are diagnosed at an advanced stage and curative surgical treatments are sometimes difficult due to the presence of peritoneal dissemination or extra-regional lymph node metastases. The long-term prognosis of curatively resected advanced gastric cancer remains unsatisfactory because of its high recurrence rate after surgery. The available chemotherapeutic reagents have only limited efficacy against these recurrent diseases. Therefore, new therapeutic strategies for advanced and recurrent gastric cancers are urgently needed.

Key words: oncolytic virus, herpes simplex virus, thrombospondin-1, gastric cancer, antiangiogenesis
Grant sponsor: Japan Society for the Promotion of Science (JSPS) Grants-in Aid for Scientific Research; **Grant numbers:** 17591433, 20591574; **Grant sponsor:** Takeda Science Foundation, Japan
DOI: 10.1002/ijc.27681
History: Received 16 Jan 2012; Accepted 1 Jun 2012; Online 22 Jun 2012
Correspondence to: Mikihito Nakamori, Second Department of Surgery, Wakayama Medical University, School of Medicine, 811-1 Kimiidera, Wakayama 641-8510, Japan, Tel.: +81-73-441-0613, Fax: +81-73-446-6566, E-mail: chamcham@wakayama-med.ac.jp

Replication-selective oncolytic herpes simplex viruses (HSVs) have emerged as a new platform for cancer therapy. Several oncolytic HSV mutants (1716, G207, NV1020 and OncoVex$^{GM\text{-}CSF}$) have already entered Phase I, II and III clinical trials for various solid tumors.[3–7] Despite the significant efficacy in preclinical models and safety in humans, however, the therapeutic benefits appear to be limited in cancer patients. It is therefore prudent to incorporate mechanisms in addition to direct oncolysis to enhance the tumor cell destruction. To this end, we have already shown that oncolytic HSVs with membrane fusion activity resulting from either genetically inserting a hyperfusogenic glycoprotein or random mutagenesis have an enhanced antitumor potency, while also exerting a synergistic effect on syncytial formation which facilitates the spread of the oncolytic virus in tumor tissue.[8–10] In addition, our collaborators have previously shown that HSV mutant G47Δ, in addition to enhanced viral replication, also possesses an immunoregulatory function, by which MHC Class I presentation was increased compared with its parent virus, G207, while maintaining the safety profile of G207.[11] This provides for the possibility of developing an enhanced cytotoxic lymphocyte response toward tumor cells and increased efficacy of the virus.

What's new?

Oncolytic virotherapy using herpes simplex virus (HSV) engineered to destroy tumor cells represents a promising new anticancer strategy. In this study, to enhance the effects of oncolytic HSV, an "armed" virus expressing human thrombospondin-1 (TSP-1), an antiangiogenic protein, was developed. The armed virus, T-TSP-1, inhibited human gastric cancer cell growth both *in vitro* and *in vivo*. The enhanced viral antitumor efficacy observed suggests that T-TSP-1 may be a useful tool in the treatment of gastric cancer.

Another problem with oncolytic virotherapy is the rapid innate immune responses that accompany viral infection, which induces the upregulation of angiogenic factors, such as vascular endothelial growth factor, and the downregulation of antiangiogenic factors, such as thrombospondin-1 (TSP-1) and thrombospondin-2 (TSP-2).[12,13] Moreover, Aghi *et al.* reported that TSP-1 reduction, accompanied with oncolytic virotherapy, induced increased angiogenesis of the residual tumor and resulted in the regrowth of tumors after oncolytic virotherapy.[12]

TSP-1 is a multifunctional 450 kDa homotrimetric glycoprotein and was originally described as a naturally occurring antiangiogenic factor and later as a potent tumor inhibitor.[14–16] The antitumor mechanisms of TSP-1 are reported to include antiangiogenesis *via* CD36,[17] induction of apoptosis,[18,19] latent transforming growth factor β (TGF-β) activation[20] and inhibition of matrix metalloproteinase 9 (MMP-9) activation.[21] TSP-1 mimetics and genes expressing them have been reported to have synergism when used with oncolytic HSV[12,22] and chemotherapeutic reagents, such as paclitaxel and cisplatin.[23] While TSP-1 is expected to have various effects that could be useful for cancer therapy, its use in infusion or injection treatments is limited because of its size and difficulty in large-scale production, and non-viral and replication-deficient viral vectors are thought to have limited success due to their poor distribution in the solid tumor mass and the tumor microenvironment.

To resolve these problems, we used replication-competent oncolytic HSVs as a vector to deliver TSP-1 to a tumor and its microenvironment, and hypothesized that, if oncolytic HSVs were combined with TSP-1, they would exert enhanced antitumor efficacy. Our viruses showed enhanced antitumor effects both *in vitro* and *in vivo via* direct antitumor and antiangiogenic mechanisms.

Material and Methods

Cell lines and viruses

Vero (Africa green monkey kidney), AZ521, MKN1, MKN28, MKN45 and MKN74 (human gastric cancer cell lines) cells were originally obtained from the RIKEN BioResource Center (Tsukuba, Japan). All of the cell lines were authenticated according to the Cell Line Verification Test Recommendations of ATCC Technical Bulletin no.8 (2008) within 3 months. TMK-1 cells, a human gastric cancer cell line, were a gift from Dr. Eiichi Tahara (Hiroshima University, Hiroshima, Japan). The TMK-1, MKN1, MKN28, MKN45 and MKN74 cells were cultured in RPMI1640 containing 10% fetal bovine serum (FBS) (GIBCO, Grand Island, NY). AZ521 cells and Vero cells were cultured in dulbecco's modified eagle medium (DMEM) containing 10% FBS. T-01 is an HSV-1-based oncolytic virus, constructed by deleting the ICP6 gene, α47 gene and both copies of the γ34.5 gene. The details of its construction have been published previously.[11] Viral stocks were prepared by releasing the virus from infected Vero cells with heparin, followed by high-speed centrifugation, as described previously.[8]

Cloning of thrombospondin-1 cDNA

Total RNA was extracted from normal human blood cells using an RNA Blood mini kit (Qiagen, Hilden, Germany), and reverse transcription PCR amplification with ReverTra Ace-α (Toyobo, Osaka, Japan). TSP-1 cDNA PCR amplification was performed with KOD plus (Toyobo). The oligonucleotide primer sequences used were follows: 5′-TA CAC ACA GGA TCC CTG CT-3′, sense, and 5′-TTA GGG ATC TCT ACA TTC GTA TTT CA-3′, antisense, for TSP-1 cDNA. The obtained human TSP-1 cDNA fragment was cloned into a cloning site of the pTA2 vector, named pTA2-TSP-1, using a TArget Clone Plus kit (Toyobo) according to the manufacturer's instructions. The sequence of obtained pTA2-TSP-1 was compared with the GenBank sequence of human TSP-1 (accession no. NM_003246) and confirmed. A 3.7-kb *EcoRV-SacII* fragment containing a human TSP-1 cDNA fragment was inserted into the *StuI-SacII* site of SV-01 to generate SV-TSP-1.

Construction of the virus

Using a bacterial artificial chromosome (BAC) and Cre/loxP and FLPe/FRT recombinase systems, oncolytic HSVs were constructed. Mutagenesis of the T-BAC plasmid was done by a two-step replacement procedure as reported in a previous study.[24,25] The T-BAC plasmid (1.5 μg) and SV-TSP-1 (150 ng) were mixed and incubated with Cre recombinase (New England BioLabs, Ipswich, MA) and were electroporated into *E. coli* ElectroMaxDH10B (Invitrogen, Carlsbad, CA) using a Gene Pulser (Bio-Rad Laboratories, Hercules, CA). The bacteria were streaked onto LB plates containing Cm (15 μg/ml) and Kan (10 μg/ml) and incubated to select clones containing the mutant BAC plasmid. Recombinant T-BAC/SV-TSP-1 was digested with *Hind* III and electrophoresed on a 0.8% SeaKem GTG Agarose Gel (Takara Bio, Shiga, Japan) in TAE buffer at 2.5 cm/V for 18 hr with High MW DNA Markers

(Invitrogen). A total of 2 μg of T-BAC/SV-TSP-1 DNA and 0.5 μg of pOG44 (Invitrogen) were transfected into Vero cells with 10 μl Lipofectamine 2000 and 5 μl of Plus Reagent (Invitrogen). Virus was grown and selected as described.[24] The progeny viruses were further selected by limiting dilution, were cloned on Vero cells and were finally designated as T-TSP-1.

In vitro immunocytochemical staining

Vero, TMK-1 and MKN74 cells were seeded in 6-well plates at 1×10^6 per well, then the cells were treated with PBS(−) and T-01 (Vero cells: multiplicity of infection (MOI) of 0.01, gastric cancer cells:MOI of 0.1) and T-TSP-1 (Vero cells:MOI of 0.01, gastric cancer cells:MOI of 0.1) after 24 hr of incubation and were incubated further at 37°C for 24 or 48 hr. Cells were fixed with 4% paraformaldehyde/PBS and washed in PBS(−) (pH 7.4), incubated with 3% hydrogen peroxide in methanol to block endogenous peroxidase, then washed in PBS(−) and incubated in protein block solution (Dako Cytomation, Glostrup, Denmark). They were incubated with an anti-human TSP-1 antibody [1:20] (R&D Systems, Minneapolis, MN). The samples were then rinsed with PBS(−), followed by incubation with Histofine Simple Stain MAX (MULTI) (Nichirei, Tokyo, Japan). Diaminobenzidine was used as a chromogen to detect the immunostaining as a brown product, and sections were counterstained with hematoxylin. Samples were observed using a Nikon ECLIPSE 80i (Nikon, Tokyo, Japan) microscope, and images were captured.

Western blotting

TMK-1 gastric cancer cells were seeded in 10-cm dish at 2×10^6 cells per dish and incubated at 37°C. After a 24 hr incubation cells were infected PBS(−) and T-01 (MOI of 1.0) and T-TSP-1 (MOI of 1.0) and incubated further at 39.5°C for 20 hr and harvested. Proteins (30 μg) were subjected to sodium dodecyl sulfate polyacrylamide gel electrophoresis (SDS-PAGE), transferred to nitrocellulose membrane (Bio-Rad) and blotted 2 hr with monoclonal mouse anti-TSP-1 antibody (diluted 1:500, R&D systems), or an hour with mouse anti-β-actin antibody (diluted 1:2000, Sigma). The membrane was then washed and blotted with an horseradish peroxidase (HRP)-conjugated anti-mouse secondary antibody (diluted 1:4000, GE healthcare, Piscataway, NJ), washed, exposed to enhanced luminol-based chemiluminescent (ECL) Plus (GE healthcare) and developed.

In vitro cytotoxicity of T-01 in gastric cancer cell lines

T-01 was used to treat gastric cancer cell lines *in vitro*. The cells were seeded on 24 well plates at 1×10^4 per well and incubated. Following a 24 hr incubation, the cells were infected with T-01 at an MOI of 0.1 and further incubated at 37°C. The number of surviving cells were measured daily using a CellTiter 96 AQueous One Solution Cell Proliferation Assay (Promega, Madison, WI) according to manufacturer's instructions, and the survival was expressed as a percentage of the PBS(−) treated control cells.

Comparison of virus yields and cytotoxicity of T-01 and T-TSP-1 *in vitro*

For virus yields studies, TMK-1 cells, which are moderately sensitive to T-01, MKN1 cells, which are only minimally sensitive to T-01, and Vero cells, were seeded on 12 well plates at 1×10^5 per well and incubated for 24 hr. Each well was infected with either T-01 or T-TSP-1 at an MOI of 0.1 (TMK-1 and MKN1 gastric cancer cells) or at an MOI of 0.01 (Vero cells) for 1 hr and further incubated at 37°C. After a 48-hr incubation, the cells scraped and lysed by three cycles of freezing and thawing. The progeny virus was titered on Vero cells by plaque assays. Each experiment was measured in triplicate. For cytotoxicity studies of T-01 and T-TSP-1, cells were seeded on 24-well plates at 1×10^4 per well and incubated for 24 hr. Each well was infected with either T-01 or T-TSP-1 at an MOI of 0.1 or 0.01, and further incubated at 37°C. The number of surviving cells was measured daily and was expressed as a percentage of the PBS(−)-treated control.

In vitro apoptosis assay

To examine the apoptotic effect of TSP-1, we performed a TUNEL assay using TMK-1 and MKN1 gastric cancer cells infected with either T-01 or TSP-1. A total of 1×10^6 TMK-1 or MKN1 cells were plated on 6-well plates and were treated with T-01 (at an MOI of 0.1), T-TSP-1 (at an MOI of 0.1) or PBS(−) (control) after a 24-hr incubation. At 48 hr after treatment, a terminal deoxynucleotidyl transferase dUTP nick end labeling (TUNEL) assay was performed using an APO-BRDU kit (BD Pharmingen, San Jose, CA) according to manufacturer's instructions, and the cells were analyzed with a FACScaliber flow cytometer and the CellQuest software program (Becton Dickinson Immunocytometry System, Franklin Lakes, NJ).

In vivo subcutaneous tumor therapy

The 6-week-old female BALB/c nu/nu mice were purchased (CLEA Japan, Tokyo, Japan). Subcutaneous tumors were generated by injecting 1×10^6 TMK-1 cells in 50-μl medium into the right flank of the mice. When subcutaneous tumors reached ~6 mm in diameter, usually 5–7 days after implantation, animals were randomized into three groups, and 20 μl of PBS(−) containing 10% glycerol, 1×10^7 pfu T-01 or the same concentration of T-TSP-1 in 20 μl PBS(−) containing 10% glycerol were inoculated into the subcutaneous tumors (Day 0). Tumor growth was determined by measuring the tumors twice a week using calipers and calculating the tumor volume as: volume = 0.5 × (long axis) × (short axis)^2 and was expressed tumor growth ratio as previous reports.[26–28] Observations were continued until 4 weeks after virus inoculation. The mice were euthanized when the tumor reached >20mm. All animal studies were conducted under the guidelines approved by the Animal Care and Use Committee of Wakayama Medical University.

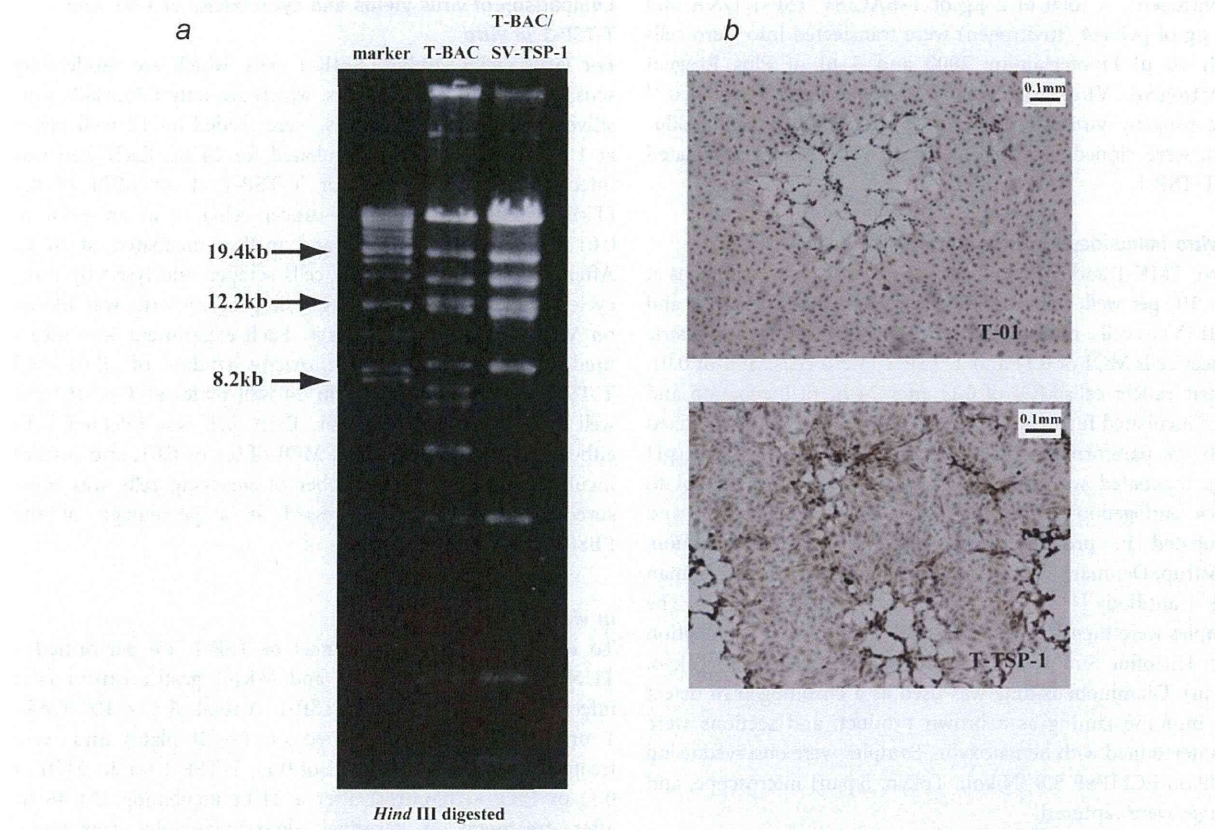

Figure 1. Verification of T-TSP-1 and TSP-1 expression in oncolytic HSV-1-infected Vero cells. (*a*) BAC plasmids were digested with *Hind* III. The digested BAC plasmids were electrophoresed, T-BAC (left) and Cre-recombinant BAC plasmid, T-BAC/SV-TSP-1 (right). (*b*) Vero cells infected with T-01 (MOI of 0.01) and T-TSP-1 (MOI of 0.01) were immunostained with an anti-TSP-1 antibody. [Color figure can be viewed in the online issue, which is available at wileyonlinelibrary.com.]

Histological examination

Animals were sacrificed on Day 7 after viral inoculation and tumor tissues were embedded in O.C.T. compound, were frozen in liquid nitrogen and stored at −80°C. Five micrometers thick sections were mounted on silanized slides (Dako Cytomation). Sections were used for HE, CD31 and TSP-1 staining. For immunohistochemical staining, samples were fixed, followed endogenous peroxidase blocking, protein blocking and were then rinsed. For CD31 staining, samples were incubated with a rat anti-CD31 antibody [1:200] (BD PharMingen), followed incubation with secondary antibody Histofine Simple Stain MAX(PO)(R) (Nichirei). For TSP-1 staining, the sections were incubated with an anti-human TSP-1 antibody [1:20] (R&D Systems Inc.), rinsed and then incubated with Histofine Simple Stain MAX(PO) (MULTI) (Nichirei). Diaminobenzidine was used as a chromogen to detect all immunostaining as a brown product, and sections were counterstained with hematoxylin. The microvessel densities (MVD) of tumors stained with an anti-CD31 antibody was measured for five individual areas with no overlap at 200-fold magnification (0.724 mm^2) for each section.

Statistical analysis

The statistical analyses were performed using Student's *t*-test. A p value < 0.05 was considered to be statistically significant. The StatView 5.0 software program (SAS institute Inc., Cary, NC) was used for all of the statistical analyses.

Results

Construction of an oncolytic herpes simplex viruses expressing thrombospondin-1

Using a BAC and Cre/loxP and FLPe/FRT recombinase systems, we generated an oncolytic HSV armed with human TSP-1, which we named T-TSP-1. This oncolytic HSV had deletions in both copies of the γ34.5 gene and in the ICP6 and α47 genes. The transgene, driven by a cytomegalovirus (CMV) promoter and with the *lacZ* gene as a marker, was inserted into the deleted ICP6 locus as previously reported.[24] The TSP-1 gene was inserted into the multicloning site of the shuttle vector SV01, and a TSP-1 expressing shuttle vector, named SV-TSP-1 was generated. Then, the recombinant BAC plasmid (T-BAC/SV-TSP-1) and T-BAC were digested with *Hind* III and electrophoresed to confirm the insertion of SV-TSP-1 (Fig. 1*a*).

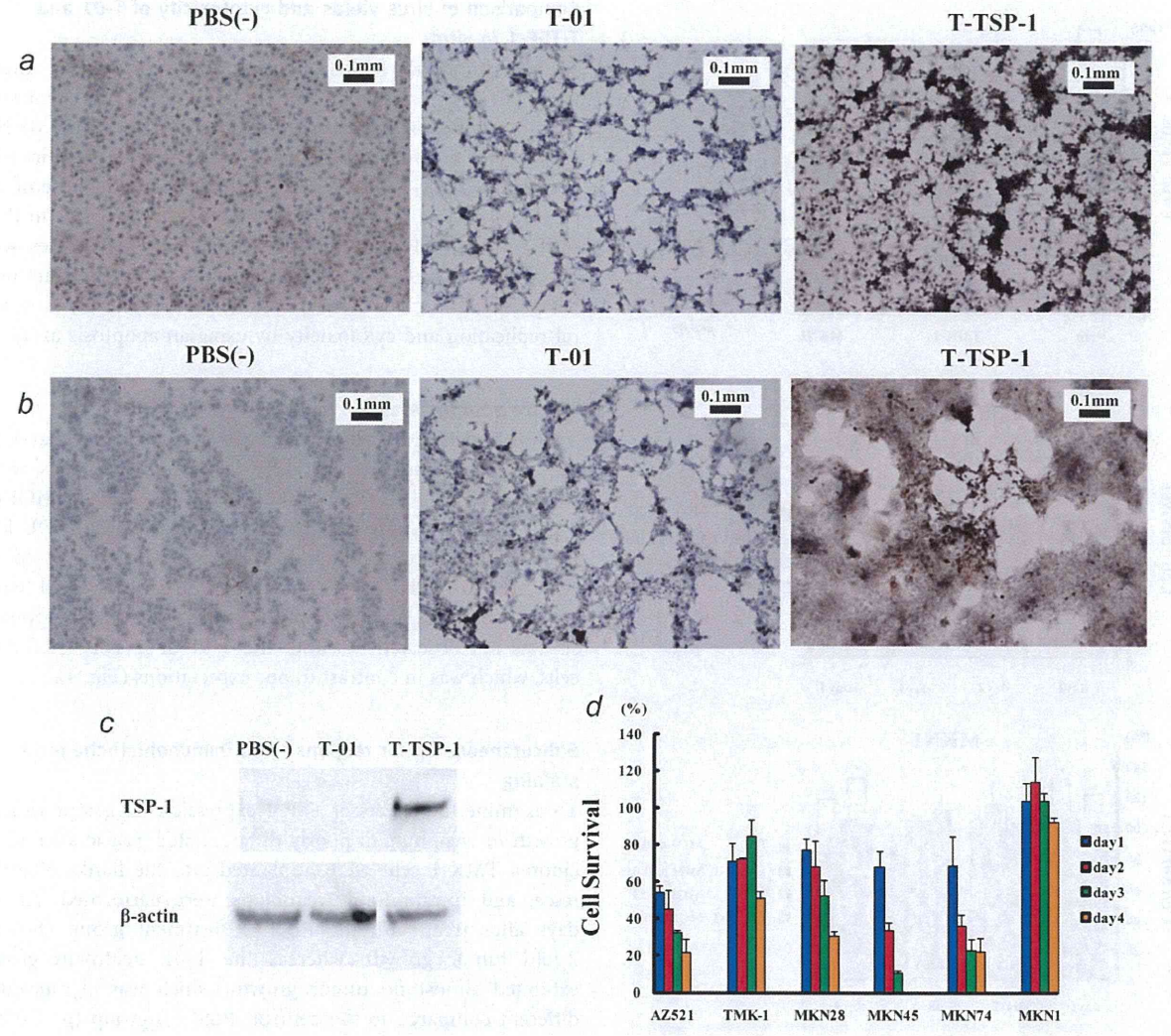

Figure 2. Immunocytochemical detection of TSP-1 and the cytotoxicity of T-01 in gastric cancer cell lines *in vitro*. Gastric cancer cells were infected with PBS(−), T-01 or T-TSP-1 and immunostained for human TSP-1 48 hr after infection. (*a*) TMK-1 cells after infection with PBS(−)(left), T-01 (middle) or T-TSP-1 (right). (*b*) MKN74 cells after infection with PBS(−)(left), T-01 (middle) or T-TSP-1 (right). (*c*) Expression of TSP-1 was confirmed by Western blotting. TMK-1 cells were infected with PBS(−) (left) or with T-01 (middle) or with T-TSP-1 (right). Note the presence of full-length TSP-1 in cells infected with T-TSP-1. (*d*) T-01 was administrated to gastric cancer cell lines *in vitro*. The cells were seeded on 24-well plates at 1×10^4 per well and were incubated for 24 hr. Following this incubation, the cells were infected with T-01 at an MOI of 0.1 and further incubated at 37°C. The number of surviving cells was measured daily and is expressed as a percentage of the PBS(−)-treated control. [Color figure can be viewed in the online issue, which is available at wileyonlinelibrary.com.]

In vitro immunocytochemical staining and Western blot analysis

To determine the activity of the virus expressing TSP-1 (T-TSP-1), Vero cells were treated with T-01 (MOI of 0.01), T-TSP-1 (MOI of 0.01) or PBS(−), and TMK-1 cells and MKN74 cells were treated with T-01 (MOI of 0.1), T-TSP-1 (MOI of 0.1) or PBS(−). Immunocytochemical staining with an anti-human TSP-1 antibody was performed 48 hr after treatment with PBS(−), T-01 or T-TSP-1. TSP-1 expression was detected in the Vero cells treated with T-TSP-1, but was not detected in Vero cells treated with T-01 (Fig. 1*b*). TSP-1 was expressed strongly in human gastric cancer cells infected with T-TSP-1, but was not expressed in gastric cancer cells treated with PBS(−) or T-01 (Figs. 2*a* and 2*b*). The expression of TSP-1 in T-TSP-1-infected Vero cells and human gastric cancer cells was confirmed. By Western blot analysis, moreover, expression of full-length TSP-1 in T-TSP-1 infected TMK-1 cells was confirmed, while TMK-1 cells infected by T-01 was not confirmed (Fig. 2*c*).

In vitro cytotoxicity of T-01 in gastric cancer cell lines

At 96 hr after infection with T-01 at an MOI of 0.1, 79% of AZ521, 49% of TMK-1, 69% of MKN28, almost all MKN45

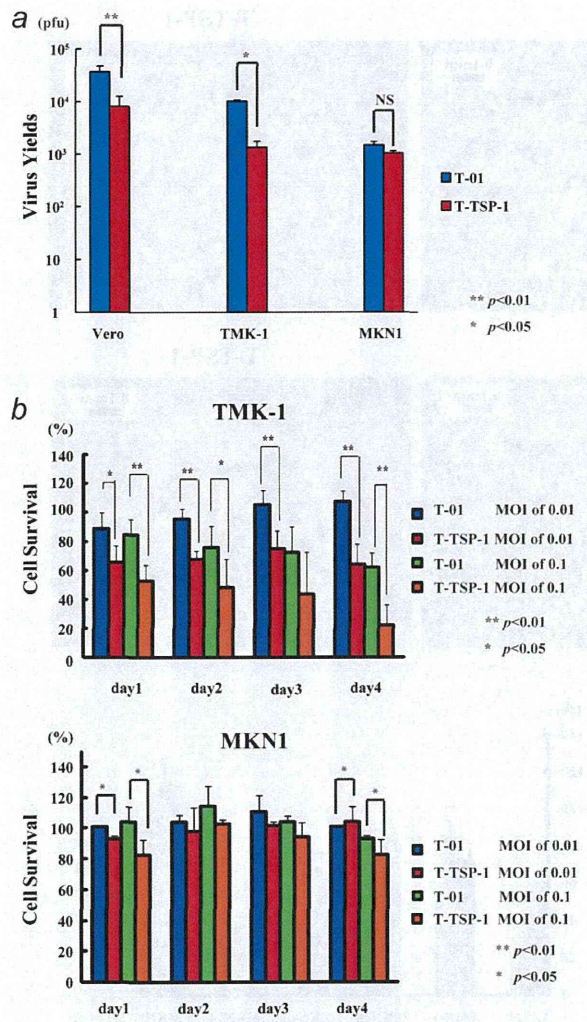

Figure 3. *In vitro* viral replication and cytotoxicity of HSVs against gastric cancer cell lines. (*a*) The *in vitro* virus yield was determined 48 hr after infection of Vero cells (1×10^5 per well) with T-01 or T-TSP-1 at an MOI of 0.01, and TMK-1 and MKN1 cells (1×10^5 per well) at an MOI of 0.1. (*b*) TMK-1 and MKN1 cells were seeded into 24-well plates at 1×10^4 per well. After a 24-hr incubation, the cells were treated with PBS(−)(control), T-01 (at an MOI of 0.01 or 0.1) or T-TSP-1 (at an MOI of 0.01 or 0.1). The number of surviving cells was quantified daily, considering control samples to be 100% viable. Bars: SE. $*p < 0.05$; $**p < 0.01$. [Color figure can be viewed in the online issue, which is available at wileyonlinelibrary.com.]

and 78% of the MKN74 cells had been killed. On the other hand, only 8% of the MKN1 cells were killed by T-01 (Fig. 2*d*). The sensitivities to T-01 were different among the human gastric cancer cell lines. Therefore, we further examined the cytotoxicity and performed a virus replication assay of T-TSP-1 or T-01, in moderate and minimally sensitive gastric cancer cell lines, TMK-1 and MKN1.

Comparison of virus yields and cytotoxicity of T-01 and T-TSP-1 *in vitro*

We determined the yields of progeny virus 48 hr after infection with each virus for 1 hr. The virus yields were not significantly different between T-TSP-1 and T-01 in the MKN1 cells. However, the virus yields of T-TSP-1 were significantly reduced in TMK-1 and Vero cells compared with those of T-01 (Fig. 3*a*). The cytotoxicity of T-TSP-1 was superior to that of T-01 in the TMK-1 cells, but neither of the viruses was effective against the MKN1 cells (Fig. 3*b*). We next examined the potential mechanism responsible for the differences in viral replication and cytotoxicity by using an apoptosis assay.

In vitro apoptosis assay

TMK-1 and MKN1 cells were plated on 6-well plates at 1×10^6 per well, and after a 24-hr incubation, the cells were treated with PBS(−), T-01 (MOI of 0.1) or T-TSP-1 (MOI of 0.1). TUNEL assays were performed using an APO-BRDU kit. In MKN1 cells, the induction of apoptosis was observed in cells treated with T-TSP-1, but not in cells treated with PBS(−) or T-01 (Fig. 4). However, in the TMK-1 cells, apoptosis was not observed in either the T-01 or T-TSP-1-infected cells, which was in contrast to our expectations (Fig. 4).

Subcutaneous tumor response and immunohistochemical staining

To examine the effects of TSP-1 expression on gastric cancer growth *in vivo*, human poorly differentiated gastric adenocarcinoma TMK-1 cells were implanted into the flanks of nude mice, and intratumoral treatments were performed. At 16 days after treatment, the PBS(−) treatment group showed 7-fold tumor growth, whereas the T-01 treatment group exhibited almost no tumor growth, which was significantly different compared to the control (PBS(−)) group ($p < 0.01$; Fig. 5*a*). Moreover, T-TSP-1 treatment group led to a significant tumor growth delay compared with T-01 treatment group ($p < 0.05$, compared with T-01; Fig. 5*a*).

Immunohistochemical staining of subcutaneous tumors treated with PBS(−), T-01 and T-TSP-1 was performed using an anti-TSP-1 antibody. No or slight TSP-1 staining was observed in tumor sections treated with PBS(−) or T-01, but strong TSP-1 staining was observed in samples from animals treated with T-TSP-1 (Fig. 5*b*). To determine whether the TSP-1-mediated inhibition of tumor growth in the different virus treatment groups reflected differences in angiogenesis, the MVD were determined. The MVD of subcutaneous tumors 7 days after treatment was determined by staining 5-μm thick frozen tumor sections with anti-CD31 antibodies, and the average densities of five independent fields were observed at a magnification of ×200. The MVD of T-01-treated tumors was significantly lower than that of PBS(−)-treated tumors ($p < 0.01$; Fig. 5*c*). In addition, that of T-TSP-1-treated tumors was significantly lower than that of T-01-treated tumors ($p < 0.05$; Fig. 5*c*). The decreased angiogenesis in tumors was thought to

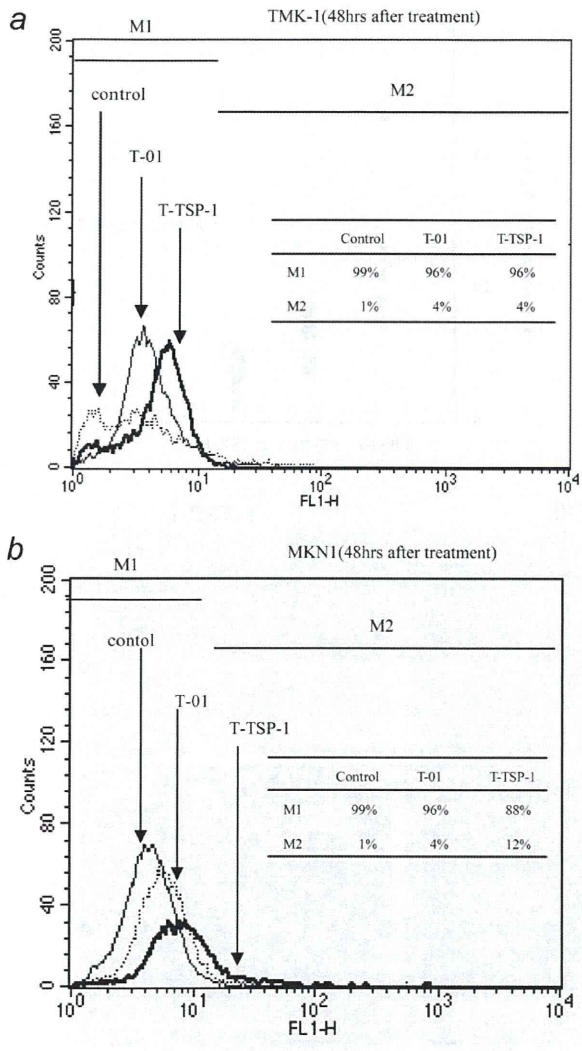

Figure 4. *In vitro* apoptosis assay of gastric cancer cells infected with oncolytic HSVs. (*a*) We performed an *in vitro* TUNEL assay using TMK-1 gastric cancer cells 48 hr after infection with PBS(−) (control), T-01 (MOI of 0.1) or T-TSP-1 (MOI of 0.1). (*b*) The results of the *in vitro* TUNEL assay of MKN-1 gastric cancer cells 48 hr after infection with PBS(−) (control), T-01 (MOI of 0.1) or T-TSP-1 (MOI of 0.1).

play an important role in the tumor growth inhibition induced by the virus.

Discussion

In this article, we described the impact of an oncolytic HSV armed with a therapeutic transgene, TSP-1. The expression of TSP-1 in cancer cells was previously reported to be repressed compared with that of normal cells.[29,30] A decreased expression of TSP-1 in cells infected with HSVs was also reported.[12,31] The administration of a TSP-1 mimetic reported enhanced the efficacy of chemotherapeutic reagents,[23] and it was also reported that the mimetic enhanced the activity of oncolytic HSVs.[12,22]

We hypothesized that an increased expression of TSP-1 in cancer cells infected with oncolytic HSVs would enhance the efficacy of the oncolytic HSVs. The whole protein and Type 1 and Type 3 repeat regions of TSP-1 have been used for anti-cancer and anti-leukemic therapy, and tumor apoptosis and inhibition of tumor angiogenesis and tumor growth were reported for these treatments.[19–21,32–34] The intact TSP-1 protein was reported to be considerably more active than the recombinant protein when injected[34] and may show more effective tumor growth inhibition than the recombinant domains of TSP-1. Therefore, in this study, we tried to compensate for the low TSP-1 expression in cells infected with oncolytic HSVs and in cancer cells in general by using a BAC system and Cre-loxP and FLP/FRT recombinase systems to arm the viruses with the intact TSP-1 gene.

We first tried to confirm the cytotoxicity of T-01 in human gastric cancer cell lines and whether the efficacy of T-01 was different in each of the gastric cancer cell lines. In the case of gastric cancer cells highly sensitive to oncolytic HSV-1 (AZ521, MKN45 and MKN74), oncolytic HSV-1 therapy alone is thought to be sufficient. On the other hand, other therapeutic modalities have to be selected for the more resistant gastric cancer cells, such as MKN1. We therefore armed the oncolytic HSV-1 to enhance its efficacy, and make it better adapted for gastric cancer cells that are only moderately sensitive to oncolytic HSV-1, for example, TMK-1.

In our *in vitro* experiments, enhanced cytotoxicity of an oncolytic HSV expressing TSP-1 was observed in TMK-1 cells compared with T-01 treatment. The results showed that the overall trend of the cell survival was increasing from Day 1 to Day 3, with a sudden decrease in Day 4 especially for TMK-1 cancer cells. This pattern may be very unusual for oncolytic HSVs mediated killing. A recent report has indicated that human gastroesophageal cancer cell lines with shorter doubling times were more susceptible to viral oncolysis and demonstrated faster cytotoxicity.[35] Some of human gastric cancer cell line such as TMK-1 and MKN1 had doubling times over 36 hr (Tsuji *et al.* unpublished data). Paradoxically, higher viral titers were achieved in human gastric cancer cell lines with longer doubling times, indicating that immediate cytotoxicity may be detrimental to ultimate viral replication. Therefore, we speculated that our phenomena *in vitro* have a close resemblance to the experimental data described previously.[35]

In terms of viral replication and apoptosis, the viral replication of T-TSP-1 was lower than that of T-01 in TMK-1 cells, but not in MKN1 cells. Moreover, the induction of apoptosis by T-TSP-1 was only observed in MKN1 cells but not in TMK-1 cells. Several studies have recently demonstrated that cancer cell apoptosis was induced by TSP-1.[19,33] Apoptosis is also a host cell defense mechanism that limits viral infection, and viral infection with HSV-1 often leads cells adjacent to HSV infected cells to apoptosis,[36] which can

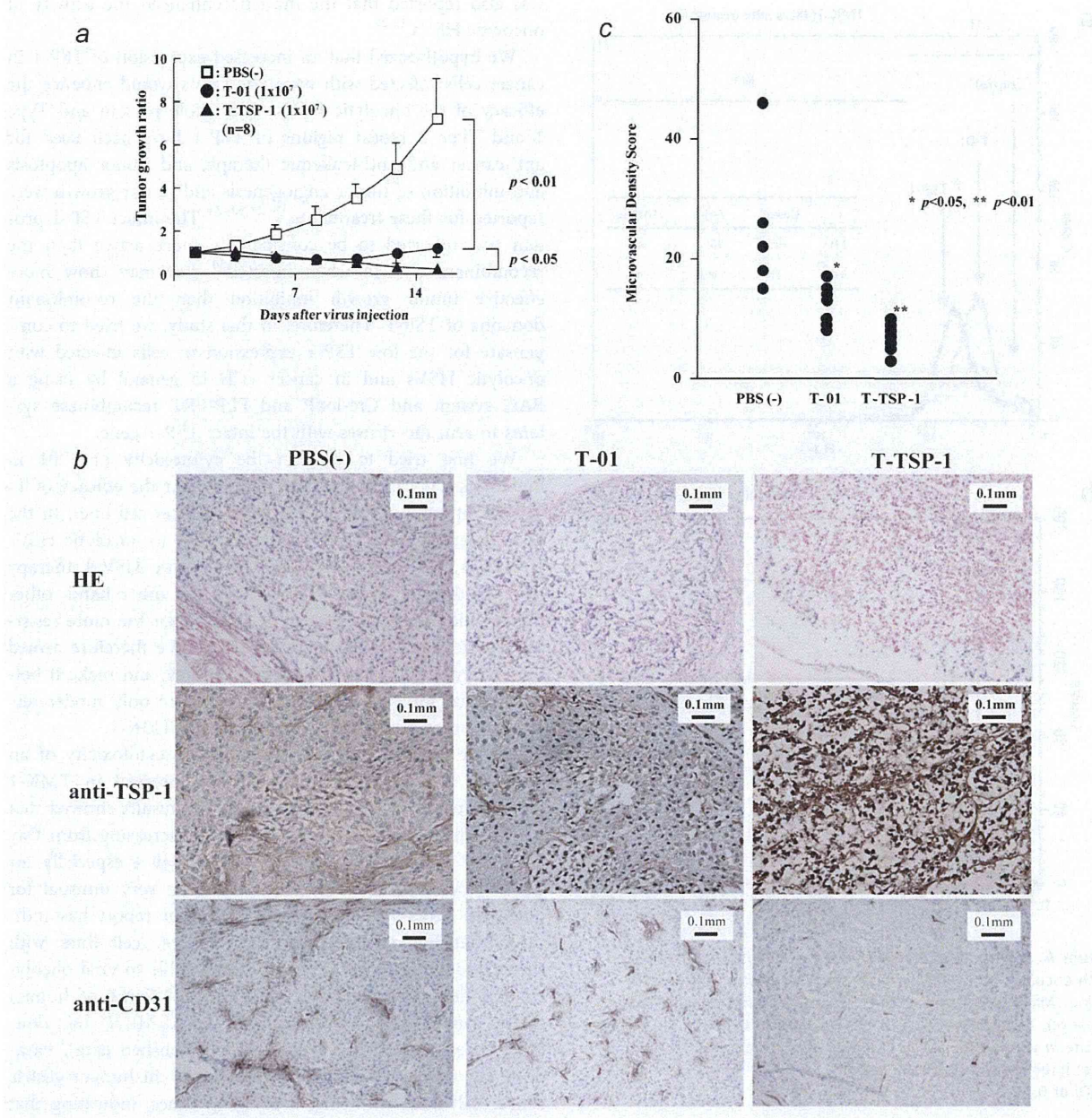

Figure 5. The efficacy of armed oncolytic HSV-1 vectors *in vivo*. (*a*) The antitumor effects of TSP-1-expressing oncolytic HSV-1s (T-TSP-1) and oncolytic HSV-1 not expressing any transgenes (T-01) was examined in BALB/c nu/nu mice bearing subcutaneous TMK-1 tumors. BALB/c nu/nu mice bearing subcutaneous TMK-1 tumors of ~6 mm in diameter were treated with intratumoral injection of PBS(−) or T-01 (1×10^7 pfu) or T-TSP-1 (1×10^7 pfu) on Day 0 ($n = 8$). The tumor growth ratio was determined by dividing tumor volume measured on the indicated week after virus injection by the tumor volume before treatment. (*b*) HE staining and immunohistochemical staining of subcutaneous tumors from mice treated with PBS(−) (left), T-01 (middle) and T-TSP-1 (right). (*c*) Subcutaneous TMK-1 tumors harvested at 7 days after treatment were stained with an anti-CD31 antibody and the MVD was evaluated for an average of five independent 200× fields. [Color figure can be viewed in the online issue, which is available at wileyonlinelibrary.com.]

attenuate the viral oncolysis. Increased viral replication of γ34.5 deficient HSV-1 was observed when used with an anti-apoptotic agent.[36] For these reasons, we speculated that the apoptotic effect of TSP-1 derived from T-TSP-1 might reduce the viral replication. It has already been reported that HSV-1 infection block apoptosis of infected cells by viral protein.[37–39] In terms of the difference of apoptosis between TMK-1 and MKN1, we hypothesized that moderately sensitive gastric

cancer cell line TMK-1 to HSV-1 was blocked apoptosis by HSV-1 infection, and lower sensitive gastric cancer cell MKN1 exhibited more apoptosis.

In diffuse-type gastric cancers, TGF-β signaling was inhibited and tumor angiogenesis was induced by repressed TSP-1 expression, which led to accelerated tumor growth. The normalization of the TGF-β pathway by inducing TSP-1 was therefore considered to be a useful potential treatment for diffuse gastric cancer.[40] Strategies using TSP-1 are also thought to be useful in the treatment of advanced cancers with defects in the TGF-β signaling pathways, such as diffuse gastric cancer. With reduced virus yields in TMK-1 cells, T-TSP-1 could also achieve a significantly better cytotoxicity than T-01. It has been reported that TSP-1 and α3β1 integrin-binding peptide from TSP-1 induced inhibition of small cell lung carcinoma cells *in vitro*.[41] We speculated that the possible mechanism of enhanced cytotoxicity of T-TSP-1 compared with T-01 *in vitro* might be induced by signal transduction from TSP-1 to α3β1 integrin. To clarify our speculation, we need to study the mechanism by which T-TSP-1 increase the cytotoxic effect in adequate tumor model.

An improved *in vivo* therapeutic effect of T-TSP-1 was also observed compared to that of T-01 in TMK-1 cells. The main mechanism of the additional effect of T-TSP-1 *in vivo* was thought to be mainly antiangiogenesis and other effects of TSP-1, such as induction of apoptosis, activation of latent TGF-β signaling[20] and inhibition of MMP-9, which has been shown to increase the invasive potential of cells,[21] were thought to be comparably weak. Further important note is that a transgenic or orthotopic model would be much more informative in comparison with a subcutaneous tumor model. In this experiment, only immune-deficient mice were assessed, and therefore, the efficacy of the treatment in immune-competent models and patients may be different. To clarify the precise mechanism of T-TSP-1, in the future, we need to use the transgenic or orthotopic tumor models in immune-competent mice and examine an anti-tumor effect *via* viral oncolysis and mechanisms including immunological aspects.

According to a previous report, the repression of TSP-1 and upregulation of TXR1 induces resistance to taxanes, which are often used in gastric cancer chemotherapy, and TSP-1 is an effector of the apoptotic response to taxane chemotherapy.[42] Synergy between 2nd generation oncolytic HSVs (G207) and taxanes in thyroid cancer therapy was confirmed in a previous study.[43] An oncolytic virus, T-TSP-1, expressing TSP-1 may therefore enhance the sensitivity of gastric cancer cells to taxanes, and combination therapy using T-TSP-1 and a taxane may achieve more enhanced synergy. Further combination studies are needed to investigate this possibility.

Finally, to the best of our knowledge, this is the first report of oncolytic HSV-1 therapy using viruses armed with TSP-1 for human gastric cancer. We showed that an oncolytic virus armed with TSP-1 enhanced the efficacy of oncolytic HSV-1 for gastric cancer cells, and that the combination of TSP-1 and oncolytic HSV-1 inhibited human gastric cancer cell growth both *in vitro* and *in vivo*. These results demonstrate that arming with TSP-1 enhances the efficacy of HSV-1 and induces apoptosis in gastric cancer cells.

References

1. Crew KD, Neugut AI. Epidemiology of gastric cancer. *World J Gastroenterol* 2006;12:354–62.
2. Hohenberger P, Gretschel S. Gastric cancer. *Lancet* 2003;362:305–15.
3. Rampling R, Cruickshank G, Papanastassiou V, et al. Toxicity evaluation of replication-competent herpes simplex virus (ICP 34.5 null mutant 1716) in patients with recurrent malignant glioma. *Gene Ther* 2000;7:859–66.
4. Markert JM, Medlock MD, Rabkin SD, et al. Conditionally replicating herpes simplex virus mutant, G207 for the treatment of malignant glioma: results of a phase I trial. *Gene Ther* 2000; 7:867–74.
5. Kemeny N, Brown K, Covey A, et al. Phase I, open-label, dose-escalating study of a genetically engineered herpes simplex virus, NV1020, in subjects with metastatic colorectal carcinoma to the liver. *Hum Gene Ther* 2006;17:1214–24.
6. Hu JC, Coffin RS, Davis CJ, et al. A phase I study of OncoVEXGM-CSF, a second-generation oncolytic herpes simplex virus expressing granulocyte macrophage colony-stimulating factor. *Clin Cancer Res* 2006;12:6737–47.
7. Kaufman HL, Kim DW, DeRaffele G, et al. Local and distant immunity induced by intralesional vaccination with an oncolytic herpes virus encoding GM-CSF in patients with stage IIIc and IV melanoma. *Ann Surg Oncol* 2010;17:718–30.
8. Nakamori M, Fu X, Meng F, et al. Effective therapy of metastatic ovarian cancer with an oncolytic herpes simplex virus incorporating two membrane fusion mechanisms. *Clin Cancer Res* 2003;9:2727–33.
9. Nakamori M, Fu X, Rousseau R, et al. Destruction of nonimmunogenic mammary tumor cells by a fusogenic oncolytic herpes simplex virus induces potent antitumor immunity. *Mol Ther* 2004;9:658–65.
10. Nakamori M, Fu X, Pettaway CA, et al. Potent antitumor activity after systemic delivery of a doubly fusogenic oncolytic herpes simplex virus against metastatic prostate cancer. *Prostate* 2004; 60:53–60.
11. Todo T, Martuza RL, Rabkin SD, et al. Oncolytic herpes simplex virus vector with enhanced MHC class I presentation and tumor cell killing. *Proc Natl Acad Sci USA* 2001;98:6396–401.
12. Aghi M, Rabkin SD, Martuza RL. Angiogenic response caused by oncolytic herpes simplex virus-induced reduced thrombospondin expression can be prevented by specific viral mutations or by administering a thrombospondin-derived peptide. *Cancer Res* 2007;67:440–4.
13. Kurozumi K, Hardcastle J, Thakur R, et al. Oncolytic HSV-1 infection of tumors induces angiogenesis and upregulates CYR61. *Mol Ther* 2008;16:1382–91.
14. Weinstat-Saslow DL, Zabrenetzky VS, VanHoutte K, et al. Transfection of thrombospondin 1 complementary DNA into a human breast carcinoma cell line reduces primary tumor growth, metastatic potential, and angiogenesis. *Cancer Res* 1994;54:6504–11.
15. Sheibani N, Frazier WA. Thrombospondin 1 expression in transformed endothelial cells restores a normal phenotype and suppresses their tumorigenesis. *Proc Natl Acad Sci USA* 1995;92: 6788–92.
16. Volpert OV, Dameron KM, Bouck N. Sequential development of an angiogenic phenotype by human fibroblasts progressing to tumorigenicity. *Oncogene* 1997;14:1495–502.
17. Dawson DW, Pearce SF, Zhong R, et al. CD36 mediates the *In vitro* inhibitory effects of thrombospondin-1 on endothelial cells. *J Cell Biol* 1997;138:707–17.
18. Manna PP, Frazier WA. CD47 mediates killing of breast tumor cells *via* Gi-dependent inhibition of protein kinase A. *Cancer Res* 2004;64:1026–36.
19. Saumet A, Slimane MB, Lanotte M, et al. Type 3 repeat/C-terminal domain of thrombospondin-1 triggers caspase-independent cell death through CD47/alphavbeta3 in promyelocytic leukemia NB4 cells. *Blood* 2005;106:658–67.

20. Yee KO, Streit M, Hawighorst T, et al. Expression of the type-1 repeats of thrombospondin-1 inhibits tumor growth through activation of transforming growth factor-β. *Am J Pathol* 2004;165:541–52.
21. Rodriguez-Manzaneque JC, Lane TF, Ortega MA, et al. Thrombospondin-1 suppresses spontaneous tumor growth and inhibits activation of matrix metalloproteinase-9 and mobilization of vascular endothelial growth factor. *Proc Natl Acad Sci USA* 2001;98:12485–90.
22. Hardcastle J, Kurozumi K, Dmitrieva N, et al. Enhanced antitumor efficacy of vasculostatin (Vstat120) expressing oncolytic HSV-1. *Mol Ther* 2009;18:285–94.
23. Campbell NE, Greenaway J, Henkin J, et al. The thrombospondin-1 mimetic ABT-510 increases the uptake and effectiveness of cisplatin and paclitaxel in a mouse model of epithelial ovarian cancer. *Neoplasia* 2010;12:275–83.
24. Fukuhara H, Ino Y, Kuroda T, et al. Triple gene-deleted oncolytic herpes simplex virus vector double-armed with interleukin 18 and soluble B7-1 constructed by bacterial artificial chromosome-mediated system. *Cancer Res* 2005;65:10663–8.
25. Liu TC, Zhang T, Fukuhara H, et al. Dominant-negative fibroblast growth factor receptor expression enhances antitumoral potency of oncolytic herpes simplex virus in neural tumors. *Clin Cancer Res* 2006;12:6791–9.
26. Fu X, Tao L, Jin A, et al. Expression of a fusogenic membrane glycoprotein by an oncolytic herpes simplex virus potentiates the viral antitumor effect. *Mol Ther* 2003;7:748–54.
27. Fu X, Tao L, Rivera A, et al. Virotherapy induces massive infiltration of neutrophils in a subset of tumors defined by a strong endogenous interferon response activity. *Cancer Gene Ther* 2011;18:785–94.
28. Fu X, Nakamori M, Tao L, et al. Antitumor effects of two newly constructed oncolytic herpes simplex viruses against renal cell carcinoma. *Int J Oncol* 2007;30:1561–7.
29. Tenan M, Fulci G, Albertoni M, et al. Thrombospondin-1 is downregulated by anoxia and suppresses tumorigenicity of human glioblastoma cells. *J Exp Med* 2000;191:1789–98.
30. Jo WS, Mizukami Y, Duerr EM, et al. Wnt signaling can repress thrombospondin-1 expression in colonic tumorigenesis. *Cancer Biol Ther* 2005;4:1361–6.
31. Choudhary A, Hiscott P, Hart CA, et al. Suppression of thrombospondin 1 and 2 production by herpes simplex virus 1 infection in cultured keratocytes. *Mol Vis* 2005;11:163–8.
32. Streit M, Velasco P, Brown LF, et al. Overexpression of thrombospondin-1 decreases angiogenesis and inhibits the growth of human cutaneous squamous cell carcinomas. *Am J Pathol* 1999;155:441–52.
33. Greenaway J, Henkin J, Lawler J, et al. ABT-510 induces tumor cell apoptosis and inhibits ovarian tumor growth in an orthotopic, syngeneic model of epithelial ovarian cancer. *Mol Cancer Ther* 2009;8:64–74.
34. Miao WM, Seng WL, Duquette M, et al. Thrombospondin-1 type 1 repeat recombinant proteins inhibit tumor growth through transforming growth factor-beta-dependent and -independent mechanisms. *Cancer Res* 2001;61:7830–9.
35. Wong J, Kelly K, Mittra A, et al. A third-generation herpesvirus is effective against gastroesophageal cancer. *J Surg Res* 2010;163:214–20.
36. Wood LW, Shillitoe EJ. Effect of a caspase inhibitor, zVADfmk, on the inhibition of breast cancer cells by herpes simplex virus type 1. *Cancer Gene Ther* 2011;18:685–94.
37. Leopardi R, Roizman B. The herpes simplex virus major regulatory protein ICP4 blocks apoptosis induced by the virus or by hyperthermia. *Proc Natl Acad Sci USA* 1996;93:9583–7.
38. Benetti L, Roizman B. Herpes simplex virus protein kinase US3 activates and functionally overlaps protein kinase A to block apoptosis. *Proc Natl Acad Sci USA* 2004;101:9411–16.
39. Ahmed M, Lock M, Miller CG, et al. Regions of the herpes simplex virus type 1 latency-associated transcript that protect cells from apoptosis *in vitro* and protect neuronal cells *in vivo*. *J Virol* 2002;76:717–29.
40. Komuro A, Yashiro M, Iwata C, et al. Diffuse-type gastric carcinoma: progression, angiogenesis, and transforming growth factor beta signaling. *J Natl Cancer Inst* 2009;101:592–604.
41. Guo N, Templeton NS, Al-Barazi H, et al. Thrombospondin-1 promotes alpha3beta1 integrin-mediated adhesion and neurite-like outgrowth and inhibits proliferation of small cell lung carcinoma cells. *Cancer Res* 2000;60:457–66.
42. Lih CJ, Wei W, Cohen SN. Txr1: a transcriptional regulator of thrombospondin-1 that modulates cellular sensitivity to taxanes. *Genes Dev* 2006;20:2082–95.
43. Lin SF, Gao SP, Price DL, et al. Synergy of a herpes oncolytic virus and paclitaxel for anaplastic thyroid cancer. *Clin Cancer Res* 2008;14:1519–28.

Oncogene (2013) **32,** 3840–3845

www.nature.com/onc

ORIGINAL ARTICLE

The critical role of cyclin D2 in cell cycle progression and tumorigenicity of glioblastoma stem cells

R Koyama-Nasu[1,4], Y Nasu-Nishimura[1,4], T Todo[2], Y Ino[2], N Saito[2], H Aburatani[3], K Funato[1], K Echizen[1], H Sugano[1], R Haruta[1], M Matsui[1], R Takahashi[1], E Manabe[1], T Oda[1] and T Akiyama[1]

Cancer stem cells are believed to be responsible for tumor initiation and development. Much current research on human brain tumors is focused on the stem-like properties of glioblastoma stem cells (GSCs). However, little is known about the molecular mechanisms of cell cycle regulation that discriminate between GSCs and differentiated glioblastoma cells. Here we show that cyclin D2 is the cyclin that is predominantly expressed in GSCs and suppression of its expression by RNA interference causes G1 arrest *in vitro* and growth retardation of GSCs xenografted into immunocompromised mice *in vivo*. We also demonstrate that the expression of *cyclin D2* is suppressed upon serum-induced differentiation similar to what was observed for the cancer stem cell marker *CD133*. Taken together, our results demonstrate that cyclin D2 has a critical role in cell cycle progression and the tumorigenicity of GSCs.

Oncogene (2013) **32,** 3840–3845; doi:10.1038/onc.2012.399; published online 10 September 2012

Keywords: cancer stem cells; cell cycle; cyclin D2; glioblastoma

INTRODUCTION

Glioblastoma is the most common primary brain tumor in adults.[1] Patients diagnosed with glioblastoma have a median survival of <1 year with generally poor responses to all therapeutic modalities. The existence of cancer stem cells responsible for tumor initiation and development has been demonstrated in a variety of tumors.[2] The discovery of glioblastoma stem cells (GSCs) was made by applying techniques for cell culture and analysis of normal neural stem cells (NSCs) to brain tumor cell populations.[3] Glioblastoma cells cultured in serum-free media supplemented with epidermal growth factor and basic fibroblast growth factor form spheres and maintain stem cell-like properties and tumorigenicity, but when grown under serum-containing culture conditions, glioblastoma cells undergo irreversible differentiation and lose their tumorigenicity.[4] Therefore, the mechanisms of maintaining the stem-like properties of GSCs have been studied extensively.

D-type cyclins are known to have critical roles in cell cycle progression.[5] Three D-type cyclins, cyclin D1, D2 and D3, are encoded by distinct genes, but show significant amino-acid similarity. Among these, cyclin D1 was first discovered and has been studied most extensively. D-type cyclins associate with partner cyclin-dependent kinases, CDK4 and CDK6, and promote phosphorylation and subsequent inactivation of the retinoblastoma tumor suppressor gene product, RB and RB-related proteins. This causes the release or de-repression of the E2F transcription factors and allows cells to enter the S phase. Dysregulation of the G1/S transition appears to be a common event in tumorigenesis.[6] Indeed, alterations in important components of the RB pathway are frequently observed in a variety of tumors, including glioblastoma.[6–8] In this study, we investigate the role of cyclin D2 in cell cycle progression and the tumorigenicity of GSCs.

RESULTS

Predominant expression of cyclin D2 in GSCs

We cultured GSCs isolated from four patients, GB1–3 and 5, under serum-free conditions that favor NSC growth.[4] Our DNA array analysis revealed that GB1 and GB2, 3 and 5 belong to the mesenchymal and proneural groups, respectively[9] (Supplementary Figure 1A). *In vitro* differentiation was induced in medium containing fetal bovine serum.[4] Differentiated GB1–3 cells proliferated more rapidly than their parental undifferentiated cells did (data not shown). By contrast, proliferation of GB5 cells was inhibited in medium containing serum (Supplementary Figure 2). Consistent with these properties, immunoblotting analysis using anti-RB antibodies revealed that RB was highly phosphorylated in differentiated GB1–3 cells and undifferentiated GB5 cells (Figure 1a). These differences may reflect the properties associated with the primary tumors from which they were derived.

To study the molecular mechanisms of cell cycle regulation in GSCs, lysates from glioblastoma cells were subjected to immunoblotting analysis with antibodies to various cyclins. We found that cyclin D2 was abundantly expressed in undifferentiated GB2, 3 and 5 cells, but was barely expressed in differentiated GB2, 3 and 5 cells, which had been cultured in serum-containing medium (Figure 1a). By contrast, cyclin D1 expression was higher in differentiated than in undifferentiated glioblastoma cells. The expression levels of cyclin D3 did not change significantly. In GB1 cells, cyclin D2 expression was not detected in either

[1]Laboratory of Molecular and Genetic Information, Institute of Molecular and Cellular Biosciences, The University of Tokyo, Bunkyo-ku, Tokyo, Japan; [2]Department of Neurosurgery, The University of Tokyo Hospital, Bunkyo-ku, Tokyo, Japan and [3]Genome Science Division, Research Center for Advanced Science and Technology, The University of Tokyo, Meguro-ku, Tokyo, Japan. Correspondence: Professor T Akiyama, Laboratory of Molecular and Genetic Information, Institute of Molecular and Cellular Biosciences, The University of Tokyo, 1-1-1, Yayoi, Bunkyo-ku, Tokyo 110-0032, Japan.
Email: akiyama@iam.u-tokyo.ac.jp
[4]These authors contributed equally to this work.
Received 22 February 2012; revised 29 June 2012; accepted 20 July 2012; published online 10 September 2012

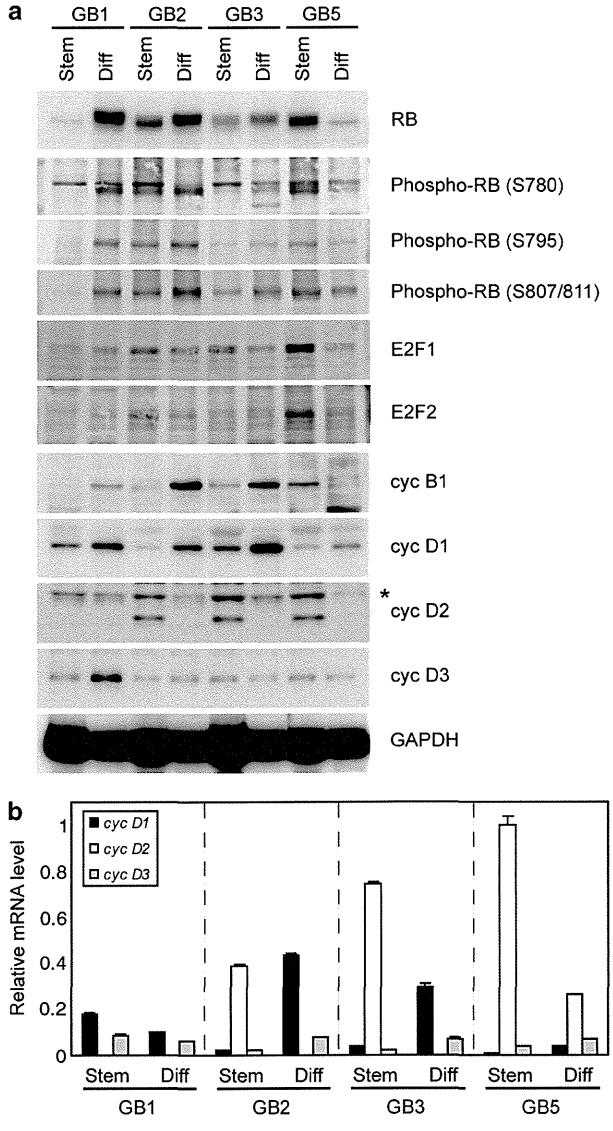

Figure 1. Predominant expression of cyclin D2 in GSCs. (**a**) Lysates from undifferentiated (stem) or differentiated (diff) GB1–3 and 5 cells were immunoblotted with antibodies to the indicated proteins. The asterisk indicates a non-specific band. (**b**) The mRNA levels of D-type cyclins in undifferentiated (stem) or differentiated (diff) GB1–3 and 5 cells were evaluated by quantitative RT–PCR. Error bars represent the s.d. ($n = 3$).

the undifferentiated or differentiated state. This may be a common feature in the mesenchymal subtype of glioblastoma (Supplementary Figure 1B). Reverse transcription–polymerase chain reaction (RT–PCR) analysis also revealed that *cyclin D2* messenger RNA (mRNA) was predominantly expressed in undifferentiated GB2, 3 and 5 cells (Figure 1b).

GSC-specific expression of cyclin D2

To further investigate the expression pattern of cyclin D2, we focused our analyses on GB2, as cyclin D2 is highly expressed and its expression is dramatically reduced by serum-induced differentiation in these cells. Time-course experiments showed that following serum addition, undifferentiated GB2 cells became attached to the bottom of the dish and formed a monolayer (Supplementary Figure 3A), as reported previously.[4] The expression levels of *cyclin D2* was significantly decreased within one day after serum addition and was completely downregulated in late-passage cells (>10 passages), similar to what was observed for the cancer stem cell marker *CD133* (Mizrak *et al.*[10]) and the NSC marker *nestin*[11] (Figure 2a, left panel). By contrast, *cyclin D1* mRNA was induced upon serum stimulation and highly expressed in late-passage cells. However, when differentiated GB2 cells (>10 passages) were cultured in serum-free conditions, cells started to form nonadherent, multicellular spheres indistinguishable from undifferentiated GSCs (Supplementary Figure 3B). Nevertheless, the expression levels of *cyclin D2* as well as *CD133* and *nestin* were not fully restored by serum deprivation (Figure 2a, right panel).

We also investigated the expression profiles of D-type cyclins in patient glioblastomas, commonly used glioma cell lines and normal human NSCs taken from a public microarray database (Figure 2b). As expected, almost all patient glioblastomas expressed substantial levels of *cyclin D2*, whereas no glioma cell line did. *Cyclin D1* was highly expressed in the glioma cell lines. Moreover, the expression of *cyclin D2* as well as *CD133* and *nestin* was not restored by serum withdrawal in the glioma cell line T98G, U251 or U87 (Figure 2c). Furthermore, either overexpression of p21 or depletion of E2F1 and/or E2F2 did not lead to the restoration of *cyclin D2* expression (Supplementary Figures 4A–D). These data are compatible with the notion that these cell lines have become differentiated under serum-containing conditions. Interestingly, *cyclin D2* and *D3*, but not *cyclin D1*, were found to be expressed in human NSCs. *Cyclin D3* and *D1* showed a reciprocal expression pattern in the glioma cell lines.

We next investigated the expression profiles of D-type cyclins in various histological grades of gliomas. The expression levels of *cyclin D2*, but not of *cyclin D1* or *D3*, were found to be significantly upregulated in glioblastomas (grade IV) compared with astrocytomas (grade II or III) and non-tumor tissues (Supplementary Figure 5 and Supplementary Table 1). Taken together, these data raise the possibility that cyclin D2 expression may be a common feature of GSCs.

Important role of cyclin D2 in cell cycle progression of GSCs

We next examined the role of cyclin D2 in cell cycle progression of GSCs using small interference RNA (siRNA). Flow-cytometric analyses of DNA content in undifferentiated GB2 cells showed that knockdown of cyclin D2, but not of cyclin D1 and/or D3, resulted in a significant increase in the fraction of cells in the G1 phase (Figure 3a, left panel). Consistent with this result, knockdown of cyclin D2 led to an increase in the amount of the hypophosphorylated form of RB, suggesting that the activity of CDK4 and/or CDK6 was suppressed and cells were arrested in the G1 phase of the cell cycle (Figure 3b, left panel). Silencing of cyclin D2 expression also caused a reduction in the level of cyclin B1, the expression of which is known to be low in the G1 phase (Figure 3b, left panel). In addition, knockdown of cyclin D2 resulted in a slight decrease in the expression levels of E2F1 and E2F2. We also observed that ectopic expression of cyclin D1 or D3 partially rescued the reduction in RB expression and phosphorylation caused by knockdown of cyclin D2. Thus, a certain amount of D-type cyclins may be required for cell cycle progression of undifferentiated GB2 cells (Supplementary Figure 6). By contrast, knockdown of cyclin D1, but not of cyclin D2 or D3, induced G1 arrest of differentiated GB2 cells cultured in serum-containing medium (Figures 3a and b, right panels). In addition, although amplification of the *cdk4* locus has been detected at a higher frequency than that of the *cdk6* locus,[7] we found that both CDK4 and CDK6 are responsible for phosphorylation of RB in undifferentiated GB2 cells (Supplementary Figures 7A and B). These results suggest that the cyclin D2–CDK4/6 complexes have an important role in cell cycle progression of undifferentiated, but not of differentiated, GSCs.

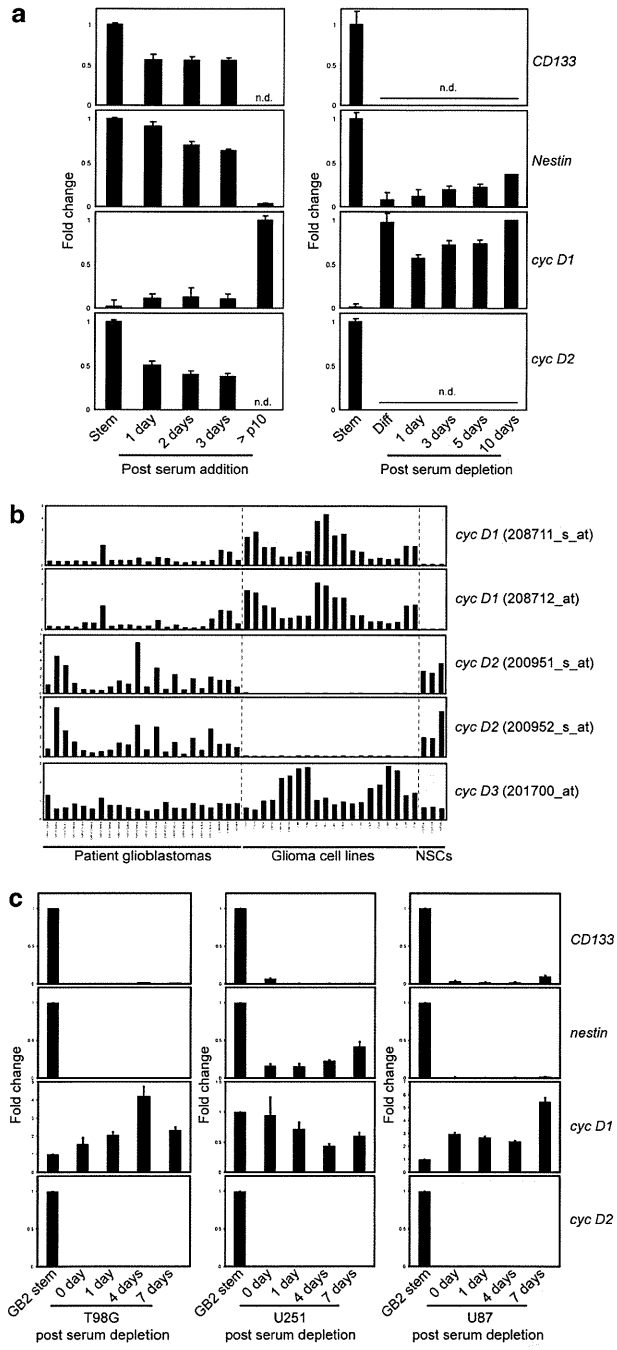

Figure 2. GSC-specific expression of *cyclin D2*. (**a**) Undifferentiated (stem) GB2 cells were cultured in medium containing serum for the indicated times (left). Differentiated (diff) GB2 cells were cultured in serum-free medium for the indicated times (right). The mRNA levels of the indicated genes were evaluated by quantitative RT–PCR and shown as fold change over mRNA levels in GB2 stem cells. Error bars represent the s.d. ($n=3$). ND means not detected. (**b**) Gene expression profiles of D-type cyclins taken from a public microarray database (GSE4536) (Lee *et al.*[4]). Data of two independent probes for *cyclin D1* and *D2*, and one probe for *cyclin D3* are shown. (**c**) The glioma cell lines T98G, U251 and U87 were cultured in serum-free medium for the indicated times. The mRNA levels of the indicated genes were evaluated by quantitative RT–PCR and shown as fold change over mRNA levels in GB2 stem cells.

Critical role of cyclin D2 in the tumorigenicity of GSCs

To clarify the significance of cyclin D2 expression in the tumorigenicity of GSCs, we transplanted GB2 cells into the frontal lobe of immunocompromised mice. As reported previously,[4] all mice transplanted with undifferentiated GB2 cells developed tumors and died within 2 months, whereas mice transplanted with differentiated GB2 cells survived over 5 months (Figure 4a). Histopathological analyses of tumor xenografts demonstrated that undifferentiated GB2 cells formed a highly invasive tumor spreading across the hemispheres, which represents an important feature of human glioblastoma (Figure 4b). RT–PCR analysis using human-specific primers demonstrated that the xenograft tumor still maintained the predominant expression of *cyclin D2* (Figure 4c and Supplementary Figure 8A). Consistent with this observation, when mice were transplanted with undifferentiated GB2 cells in which cyclin D2 expression was stably repressed by lentivirus-delivered short hairpin RNAs (shRNAs) (Supplementary Figures 8B and C), they survived significantly longer than those transplanted with undifferentiated GB2 cells infected with control lentivirus (Figure 4a). By contrast, overexpression of cyclin D2 did not restore *CD133* and *nestin* expression, as well as tumorigenicity of differentiated GB2 cells (Supplementary Figures 9A-C). These results suggest that cyclin D2 has a critical role in the tumorigenicity of GSCs.

DISCUSSION

A number of molecular studies have identified critical genetic events in glioblastoma, including the following: dysregulation of growth factor signaling; activation of the phosphatidylinositol-3-OH kinase pathway; and inactivation of the p53 and RB pathways.[7,8] Among those three core pathways, the RB pathway is obviously the most important for the regulation of G1/S progression.[6] Actually, 78% of glioblastomas are shown to harbor RB pathway aberrations, such as deletion of the *cdkn2a/cdkn2b* locus, amplification of the *cdk4* locus and deletion or inactivating mutations in *RB1* (Cancer Genome Atlas Research Network[7]). Importantly, amplification of the *cyclin D2* locus is also reported.[7] In this study, we have shown that cyclin D2 is the most abundantly expressed cyclin in GSCs among the three D-type cyclins. Moreover, suppression of cyclin D2 expression by RNA interference caused G1 arrest *in vitro* and growth retardation of GSCs xenografted into immunocompromised mice *in vivo*. Altogether, these data suggest the critical role of cyclin D2 in cell cycle progression and the tumorigenicity of GSCs.

Tumor cells in culture are valuable for studying the mechanisms of tumorigenesis. Growth media containing serum have been used for maintaining a variety of cancer cells, including glioblastoma. However, it has been shown that serum causes irreversible differentiation of GSCs.[4] Differentiated GSCs have gene expression profiles that are different from those of their parental GSCs and NSCs, and are neither clonogenic nor tumorigenic.[4] Our study shows that cyclin D2 expression is silenced when GSCs are cultured in the presence of serum. We also found that cyclin D1 expression is enhanced during serum-induced differentiation of GSCs. These results explain why commonly used glioblastoma cell lines abundantly express cyclin D1, but not cyclin D2.

It has been shown that GSCs and NSCs share similar properties such as the potential for self-renewal and differentiation.[12] Intriguingly, cyclin D2 has been reported to be the only D-type cyclin expressed in adult mouse NSCs.[13,14] Thus, it is interesting to speculate that the predominant expression of cyclin D2 in GSCs may be the reflection of the property associated with adult NSCs. It is possible that transcription factors that are important for the maintenance of the stem cell state may also be involved in cyclin D2 expression. It may also be possible that DNA

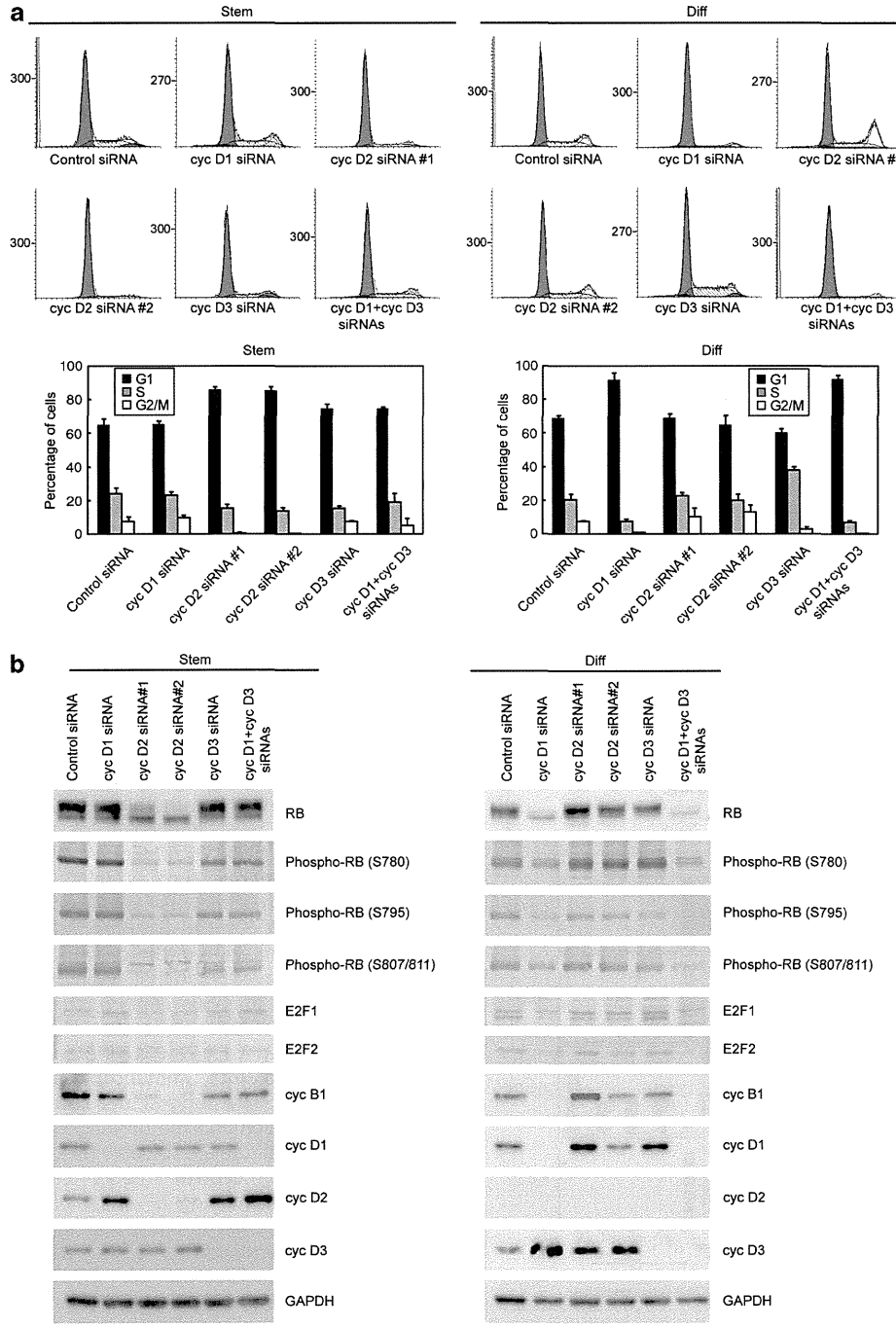

Figure 3. Important role of cyclin D2 in cell cycle progression of GSCs. (**a**) Undifferentiated (stem) (left) or differentiated (diff) (right) GB2 cells were transfected with siRNAs targeting D-type cyclins. After 72 h, cells were fixed, stained with propidium iodide and analyzed by flow cytometry for DNA content. The *x* axis represents DNA content and the *y* axis the number of cells (upper). The bar graph represents the percentages of cells in G1, S and G2/M (lower). Error bars represent the s.d. ($n = 3$). (**b**) Undifferentiated (stem) (left) or differentiated (diff) (right) GB2 cells were transfected with siRNAs targeting D-type cyclins. After 72 h, lysates were immunoblotted with antibodies to the indicated proteins.

methylation and/or mRNA stabilization by alternative cleavage- and polyadenylation-mediated shortening of 3′-UTR are involved in the alteration in cyclin D2 expression.[15]

It is important to define reliable markers that are expressed in cancer stem cells. Overexpression of cyclin D1 has been implicated in the pathogenesis of various human cancers.[5,6,16] However, our results raise the possibility that cyclin D2, rather than cyclin D1, could be a novel prognostic marker for glioblastoma. Hence, it is intriguing to perform univariate and multivariate analyses to compare the expression levels of cyclin D2 with tumorigenic capacity and tumor invasiveness.

As cancer stem cells are considered to be responsible for tumor initiation and development, GSCs may be promising targets for the therapy of glioblastoma. We therefore speculate that inhibitors

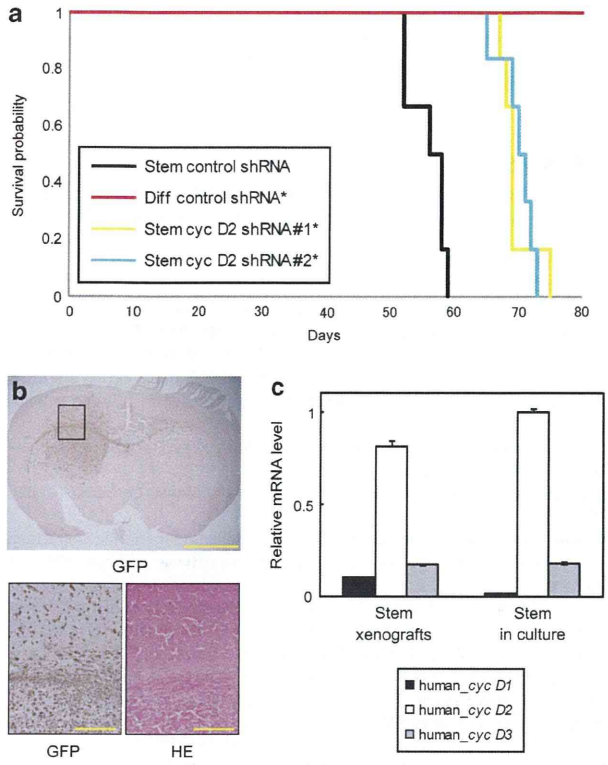

Figure 4. Critical role of cyclin D2 in the tumorigenicity of GSCs. (**a**) Undifferentiated (stem) or differentiated (diff) GB2 cells were infected with lentivirus harboring an shRNA targeting cyclin D2. After 1 week, cells were transplanted into the frontal lobe of immunocompromised mice. $*P = 0.0006$ with comparison to stem control shRNA. (**b**) Histopathological analysis of representative tumor xenograft. Undifferentiated GB2 cells were infected with control lentivirus expressing GFP and transplanted into immunocompromised mice. GFP immunostaining (distribution of tumor cells) and hematoxylin and eosin (HE) staining are shown. Scale bars represent 2 mm (upper) and 200 μm (lower). (**c**) The mRNA levels of D-type cyclins in undifferentiated (stem) GB2 xenografts and undifferentiated (stem) GB2 cells in culture were evaluated by quantitative RT–PCR using human-specific primers. Error bars represent the s.d. ($n = 3$).

that block the expression of cyclin D2 could have a growth inhibitory effect on GSCs.

MATERIALS AND METHODS

Tumor specimens and primary tumor cultures

Following informed consent, tumor samples classified as primary glioblastoma were obtained from patients undergoing surgical treatment at the University of Tokyo Hospital as approved by the Institutional Review Board. Tumors were washed, and mechanically and enzymatically dissociated into single cells. Tumor cells were cultured in Neurobasal medium (Life Technologies, Carlsbad, CA, USA) containing B27 supplement minus vitamin A (Life Technologies), epidermal growth factor and basic fibroblast growth factor (20 ng/ml each; Wako Pure Chemical Industries, Osaka, Japan). For *in vitro* differentiation, tumor cells were cultured in Dulbecco's modified Eagle's medium/F-12 medium (Life Technologies) containing 10% fetal bovine serum. Cell viability was assessed using the CellTiter-Glo Luminescent Cell Viability Assay (Promega, Madison, WI, USA).

Antibodies

Mouse monoclonal antibodies to cyclin B1, E2F1 and α-tubulin were obtained from Santa Cruz Biotechnology (Santa Cruz, CA, USA). Mouse monoclonal antibodies to cyclin D1, D2, D3 and RB were from BD Biosciences (Billerica, MA, USA). Mouse monoclonal antibody to glyceraldehyde-3-phosphate dehydrogenase (GAPDH) was from Millipore (Bedford, MA, USA). Rabbit polyclonal antibodies to E2F2 and green fluorescence protein (GFP) were from Santa Cruz Biotechnology. Rabbit pAbs to phospho-RB S780, S795 and S807/811 were from Cell Signaling Technology (Danvers, MA, USA).

Immunoblotting

Cells were lysed in lysis buffer (50 mM Tris-HCl, pH 7.5, 250 mM NaCl, 0.1% Triton X-100, 1 mM dithiothreitol, 1 mM EDTA, 50 mM NaF, 0.1 mM Na_3VO_4 and protease inhibitors). Lysates were fractionated by sodium dodecyl sulfate–polyacrylamide gel electrophoresis and transferred to a polyvinylidene difluoride membrane (Immobilon-P; Millipore). The membrane was subjected to immunoblot analysis using horseradish peroxidase-conjugated donkey anti-rabbit immunoglobulin G (GE Healthcare, Pittsburgh, PA, USA) or sheep anti-mouse immunoglobulin G (GE Healthcare) as a secondary antibody. Visualization was performed using the Enhanced Chemiluminescence Plus Western Blotting Detection System (GE Healthcare) and LAS-4000EPUVmini Luminescent Image Analyzer (GE Healthcare).

Quantitative RT–PCR

Total RNA was extracted using NucleoSpin RNA Clean-up kit (Takara Bio Inc., Shiga, Japan) and reverse-transcribed into cDNA using ReverTra Ace qPCR RT Kit (Toyobo Life Science, Osaka, Japan). Real-time PCR was performed using LightCycler480 SYBR Green I Master and a LightCycler480 Instrument (Roche, Indianapolis, IN, USA). The results were normalized with the detected value for *GAPDH* or *ACTB*. Primers used in RT–PCR were as follows: *GAPDH* forward (5′-GCACCGTCAAGGCTGAGAAC-3′), *GAPDH* reverse (5′-TGGTGAAGACGCCAGTGGA-3′); *CD133* forward (5′-AGTGG CATCGTGCAAACCTG-3′), *CD133* reverse (5′-CTCCGAATCCATTCGACGA TAGTA-3′); *nestin* forward (5′-GAGGTGGCCACGTACAGG-3′), *nestin* reverse (5′-AAGCTGAGGGAAGTCTTGGA-3′); *cyclin D1* forward (5′-TGTCCTACT ACCGCCTCACA-3′), *cyclin D1* reverse (5′-CAGGGCTTCGATCTGCTC-3′); *cyclin D2* forward (5′-GGACATCCAACCCTACATGC-3′), *cyclin D2* reverse (5′-CGCACTTCTGTTCCTCACAG-3′); and *cyclin D3* forward (5′-GCTTAC TGGATGCTGGAGGTA-3′), *cyclin D3* reverse (5′-AAGACAGGTAGCGATCCAG GT-3′). Human-specific primers were as follows: *ACTB* forward (5′-CGTCACC AACTGGGACGACA-3′), *ACTB* reverse (5′-CTTCTCGCGGTTGGCCTTGG-3′); *cyclin D1* forward (5′-ACTACCGCCTCACACGCTTC-3′), *cyclin D1* reverse (5′-CTTGACTCCAGCAGGGCTTC-3′); *cyclin D2* forward (5′-ATCACCAACAC AGACGTGGA-3′), *cyclin D2* reverse (5′-TGCAGGCTATTGAGGAGCA-3′); and *cyclin D3* forward (5′-TACACCGACCACGCTGTCT-3′), *cyclin D3* reverse (5′-GAAGGCCAGGAAATCATGTG-3′). Mouse-specific primers were as follows: *ACTB* forward (5′-GGATGCAGAAGGAGATTACTGC-3′), *ACTB* reverse (5′-CCACCGATCCACACAGAGCA-3′).

RNA interference

The stealth siRNA oligonucleotide sequences were 5′-CCACAGAUGUGAA-GUUCAUUUCCAA-3′ (cyclin D1), 5′-UGCUCCUCAAUAGCCUGCAGCAGUA-3′ (cyclin D2#1), 5′-UGACGGAUCCAAGUCGGAGGAUGAA-3′ (cyclin D2#2), 5′-AACUACCUGGAUCGCUACCUGUCUU-3′ (cyclin D3), 5′-GGGAGAUCA AGGUAACCCUGGUGUU-3′ (CDK4) and 5′-ACCGAGUAGUGCAUCGCGAU CUAAA-3′ (CDK6) (Life Technologies). Negative control stealth siRNA with medium GC content was purchased from Life Technologies. The silencer select siRNA oligonucleotide sequences were 5′-GGACCUUCGUAGCAUUG CATT-3′ (E2F1) and 5′-AGACAGUGAUUGCCGUCAATT-3′ (E2F2) (Life Technologies). Negative control silencer select siRNA was purchased from Life Technologies. Transfection of siRNA was performed using Lipofectamine RNAiMAX transfection reagent (Life Technologies). shRNAs targeting cyclin D2 were designed to harbor the same target sequences.

Flow cytometry

Cells were trypsinized, fixed in 70% ethanol and then stained with propidium iodide (Sigma, St Louis, MO, USA). Cells were passed through a FACSCalibur instrument (BD Biosciences) and the data were analyzed using the ModFit LT software (Verity Software House, Topsham, ME, USA).

Lentivirus production

Lentiviral vector CS-RfA-CG harboring an shRNA driven by the H1 promoter or CSII-CMV-RfA-IRES2-Venus harboring a cDNA driven by the CMV promoter was transfected with the packaging vectors pCAG-HIV-gp and pCMV-VSV-G-RSV-Rev into 293FT cells using Lipofectamine 2000 Transfection Reagent (Life Technologies). All plasmids were kindly provided by H

Miyoshi (RIKEN BioResource Center, Ibaraki, Japan). Viral supernatant was purified by ultracentrifugation at 25 000 r.p.m. for 90 min (SW28 rotor, Beckman Coulter, Brea, CA, USA). Infection efficiency was monitored by GFP expression as it is driven by the CMV promoter.

Intracranial xenografts

At 1 week after lentivirus infection, 1×10^4 cells were injected stereotactically into the right frontal lobe of 5-week-old nude mice (BALB/cAJcl-*nu/nu*; CLEA Japn Inc., Tokyo, Japan), following administration of general anesthesia ($n = 6$). The injection coordinates were 2 mm to the right of the midline, 1 mm anterior to the coronal suture and 3 mm deep. Mice were monitored for 6 months. Survival of mice was evaluated by Kaplan–Meier analysis. *P*-value was calculated using a log-rank test. Tumors were histologically analyzed after hematoxylin and eosin staining. Tumor distribution was analyzed by GFP immunostaining. All animal experimental protocols were performed in accordance with the politics of the Animal Ethics Committee of the University of Tokyo.

Immunohistochemistry

Samples were fixed in 3.7% buffered formalin, dehydrated and embedded in paraffin. Sections (6 μm) were rehydrated, and endogenous peroxidases were blocked by incubation in 0.3% H_2O_2 for 30 min. The primary antibody was detected using the VECTASTAIN ABC kit (Vector Laboratories, Burlingame, CA, USA). Slides were lightly counterstained with hematoxylin.

Microarray data

The expression profiles of undifferentiated GB1–3 and 5 cells were generated on the Affymetrix GeneChip HG-U133 Plus 2.0 microarray platform (Affymetrix, Santa Clara, CA, USA). The expression profiles of 15 GSCs were taken from the Gene Expression Omnibus database GSE7181 and GSE8049 (Lottaz *et al.*[9]).Data were analyzed using the software program GenePattern. The expression profiles of D-type cyclins in various histological grades of glioma were taken from GSE4290 (Sun *et al.*[17]). Data were analyzed using the software program R. *P*-value was calculated using a pairwise Wilcoxon's test. The expression profiles of D-type cyclins in patient glioblastomas, glioma cell lines and normal NSCs were taken from GSE4536 (Lee *et al.*[4]).

CONFLICT OF INTEREST

The authors declare no conflict of interest.

ACKNOWLEDGEMENTS

This work was supported by Research Program of Innovative Cell Biology by Innovative Technology (Integrated Systems Analysis of Cellular Oncogenic Signaling Networks), Grants-in-Aid for Scientific Research on Innovative Areas (Integrative Research on Cancer Microenvironment Network), Takeda Science Foundation and in part by Global COE Program (Integrative Life Science Based on the Study of Biosignaling Mechanisms), MEXT, Japan.

REFERENCES

1 Furnari FB, Fenton T, Bachoo RM, Mukasa A, Stommel JM, Stegh A *et al.* Malignant astrocytic glioma: genetics, biology, and paths to treatment. *Genes Dev* 2007; **21**: 2683–2710.
2 Alison MR, Lim SM, Nicholson LJ. Cancer stem cells: problems for therapy? *J Pathol* 2011; **223**: 147–161.
3 Singh SK, Clarke ID, Terasaki M, Bonn VE, Hawkins C, Squire J *et al.* Identification of a cancer stem cell in human brain tumors. *Cancer Res* 2003; **63**: 5821–5828.
4 Lee J, Kotliarova S, Kotliarov Y, Li A, Su Q, Donin NM *et al.* Tumor stem cells derived from glioblastomas cultured in bFGF and EGF more closely mirror the phenotype and genotype of primary tumors than do serum-cultured cell lines. *Cancer Cell* 2006; **9**: 391–403.
5 Sherr CJ, Roberts JM. Living with or without cyclins and cyclin-dependent kinases. *Genes Dev* 2004; **18**: 2699–2711.
6 Sherr CJ, McCormick F. The RB and p53 pathways in cancer. *Cancer Cell* 2002; **2**: 103–112.
7 Cancer Genome Atlas Research Network. Comprehensive genomic characterization defines human glioblastoma genes and core pathways. *Nature* 2008; **455**: 1061–1068.
8 Parsons DW, Jones S, Zhang X, Lin JC, Leary RJ, Angenendt P *et al.* An integrated genomic analysis of human glioblastoma multiforme. *Science* 2008; **321**: 1807–1812.
9 Lottaz C, Beier D, Meyer K, Kumar P, Hermann A, Schwarz J *et al.* Transcriptional profiles of CD133 + and CD133 − glioblastoma-derived cancer stem cell lines suggest different cells of origin. *Cancer Res* 2010; **70**: 2030–2040.
10 Mizrak D, Brittan M, Alison MR. CD133: molecule of the moment. *J Pathol* 2008; **214**: 3–9.
11 Lendahl U, Zimmerman LB, McKay RD. CNS stem cells express a new class of intermediate filament protein. *Cell* 1990; **60**: 585–595.
12 Sanai N, Alvarez-Buylla A, Berger MS. Neural stem cells and the origin of gliomas. *N Engl J Med* 2005; **353**: 811–822.
13 Kowalczyk A, Filipkowski RK, Rylski M, Wilczynski GM, Konopacki FA, Jaworski J *et al.* The critical role of cyclin D2 in adult neurogenesis. *J Cell Biol* 2004; **167**: 209–213.
14 Walzlein JH, Synowitz M, Engels B, Markovic DS, Gabrusiewicz K, Nikolaev E *et al.* The antitumorigenic response of neural precursors depends on subventricular proliferation and age. *Stem Cells* 2008; **26**: 2945–2954.
15 Mayr C, Bartel DP. Widespread shortening of 3'UTRs by alternative cleavage and polyadenylation activates oncogenes in cancer cells. *Cell* 2009; **138**: 673–684.
16 Zhang X, Zhao M, Huang AY, Fei Z, Zhang W, Wang XL. The effect of cyclin D expression on cell proliferation in human gliomas. *J Clin Neurosci* 2005; **12**: 166–168.
17 Sun L, Hui AM, Su Q, Vortmeyer A, Kotliarov Y, Pastorino S *et al.* Neuronal and glioma-derived stem cell factor induces angiogenesis within the brain. *Cancer Cell* 2006; **9**: 287–300.

Supplementary Information accompanies the paper on the Oncogene website (http://www.nature.com/onc)